Mechanism and Machine Theory 184 (2023) 105297

Contents lists available at ScienceDirect

Mechanism and Machine Theory

journal homepage: www.elsevier.com/locate/mechmt

A geometric and analytic technique for the determination of the instantaneous screw axes in single-DOF spatial mechanisms

Raffaele Di Gregorio *

Department of Engineering, University of Ferrara, Via Saragat,1, 44122 Ferrara, Italy

ARTICLE INFO

Keywords:
Spatial mechanisms
Kinematics
Velocity analysis
Instantaneous screw axis

ABSTRACT

In single-degree-of-freedom (single-DOF) mechanisms, the location of the instantaneous screw axes (ISAs) of the relative motions between any two links depends only on the mechanism configuration. In the literature, this property together with the Aronhold-Kennedy (AK) theorem was exploited to devise geometric and analytic techniques that determine ISAs in planar mechanisms, where the ISAs are located by the instant centers (ICs). Despite the fact that an extended Aronhold-Kennedy (EAK) theorem has been demonstrated for spatial mechanisms, too, since 1959, the spatial counterpart of these techniques has not been proposed, yet. Relating ISA locations to the mechanism configuration is important during the mechanism design and provides a deeper comprehension of the mechanism motion by disclosing the role each link plays. Here, a geometric and analytic technique based on the EAK theorem is presented for the ISA determination in single-DOF spatial mechanisms. The proposed method is indeed the extension to spatial mechanisms of those techniques used for the IC determination in planar mechanisms. The effectiveness of the proposed technique is also illustrated through two relevant case studies.

1. Introduction

The vast majority of single-DOF mechanisms have time-independent (scleronomic) constraints that are either holonomic constraints or non-holonomic constraints whose dependence on motion-variables' rates is linear (i.e., they are first-order non-holonomic constraints) [1]. If a mechanism has only one DOF, these types of scleronomic constraints make the ratios between any two motion-variables' rates, named velocity (or influence) coefficients (VCs), depend only on the mechanism configuration. In addition, the analytic/geometric expression of a VC only depends on the instantaneous screw axes (ISAs) of three relative motions, one between the two links the two motion variables refer to, and the remaining two between either of these two links and a third link of the mechanism, which usually is chosen coincident with the mechanism frame. As a consequence, the ISA locations only depend on the mechanism configuration in single-DOF mechanisms with these types of scleronomic constraints. Hereafter, for the sake of conciseness, the phrase "single-DOF mechanism" will refer to a single-DOF mechanism with these types of scleronomic constraints.

Since the ISAs pertain to the links' velocity fields, expressing the constraints between two links, say links i and j (see Fig. 1), joined by a kinematic pair, through geometric conditions on the ISA, hereafter named ISA_{ji}, of the relative motion between links j and i is possible both for holonomic and first-order non-holonomic constraints. Therefore, in single-DOF mechanisms, a fully geometric analysis that relates the ISA locations to the mechanism configuration is always possible. Such a geometric approach is relevant during

* Corresponding author.
E-mail address: raffaele.digregorio@unife.it.

https://doi.org/10.1016/j.mechmachtheory.2023.105297
Received 20 December 2022; Received in revised form 14 February 2023; Accepted 14 February 2023

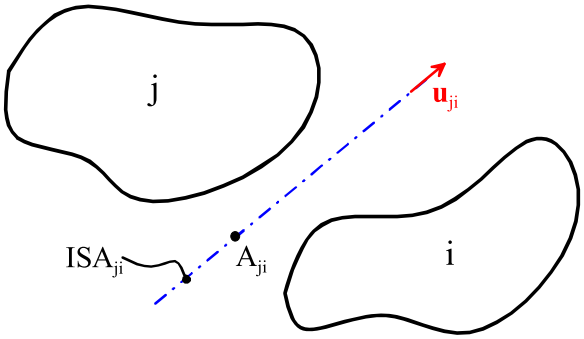

Fig. 1. System of two bodies whose relative motion is a helical motion: notations.

the mechanism design.

For planar single-DOF mechanisms where the ISAs are located by the instant centers (ICs), the demonstration [2,3] of the Aronhold-Kennedy (AK) theorem allowed the proposition of geometric and analytic techniques [4–10] that determine the IC positions by taking into account only the mechanism configuration. For spatial single-DOF mechanisms, an extended Aronhold-Kennedy (EAK) theorem[1] has been demonstrated since 1959 [11] and better detailed in the next years [12–17]. Nevertheless, in the literature, the proposed general techniques for the ISA determination [18,19,20] in spatial single-DOF mechanisms pass through the velocity analysis solution, thus loosing the advantages of a purely geometric approach, and those geometric techniques conceived for planar mechanisms have not been extended to the spatial case yet, even though some particular cases [21–25] have been geometrically analyzed.

In particular, Suh [18] differentiated the matrix relationship between homogeneous coordinates of points and introduced the "instant pitch" to obtain what he called "velocity matrix of instant pitch", which contains the coordinates of one ISA-line point, the components of the ISA-line's unit-vector and the "instant pitch" in quadratic expressions appearing in the entries of this matrix; then, he introduced such matrix type in the velocity analysis of the relative motion between two rigid bodies connected by particular binary links to obtain standard blocks to assemble according to the topology of the mechanism to analyze. In the analysis of a mechanism, this procedure must be repeated for each relative motion, whose ISA must be determined, and, anyway, it is not able to find both the relationship among the computed ISAs and the relationship between the ISAs and the mechanism's geometric constants.

In [19], Valderrama-Rodriguez et al. showed that the EAK theorem is basically the application of the Killing and Klein forms to the equation that relates the velocity states of three bodies regardless if they are free to move in the space or they form part of a kinematic chain. Then, they exploited this result to conceive a technique for determining ISAs that writes the screw associated to the sought-after ISA as a linear combination of the screws corresponding to the kinematic pairs of the kinematic chains that simultaneously connect the two links, whose relative motion is associated to the sought-after ISA, and, successively, solves the resulting system of equations by using the orthogonal annihilators with respect to the Killing and the Klein forms of the subspaces generated by the set of screws appearing in the written linear combinations. Since such linear combinations coincide with the ones that are usually written for the velocity analysis of a mechanism considered as a combination of simultaneous connections between two rigid bodies, their technique can be considered the screw-based version of the above-commented matrix-based technique presented by Suh in [18], with which it shares the above-highlighted drawbacks. Later the same authors, in [20], presented another technique that, firstly, writes the velocity-analysis equations as loop equations and solve them, and, then, uses the obtained results to compute the sought-after ISA by means of one of the linear combinations of screws used in their previous technique. This new technique is more direct of their previous one, but still keeps the above-highlighted drawbacks.

In this paper, firstly, the demonstration of the EAK theorem is revisited to reformulate the analytic relationships that accompany the geometric condition stated therein and a corollary of the EAK theorem is added. Secondly, the analytic and geometric conditions on the ISA_{ji} due to each of the possible kinematic pairs present in spatial mechanisms are reminded/deduced. Then, all these tools are combined into a general geometric and analytic procedure for the determination of all the ISAs in single-DOF spatial mechanisms. Finally, the proposed procedure is applied to two relevant case studies. The presented procedure is the spatial counterpart of the one used for the IC determination in single-DOF planar mechanisms. As far as this author is aware, even though the background concepts involved in the formulation of the proposed approach are known, their combination into a self-standing procedure for the ISA determination is novel.

The paper is organized as follows. Section 2 revisits the EAK theorem, states/proves the new corollary, reminds the geometric conditions on the ISA_{ji} due to the kinematic pairs, and presents the novel procedure for the ISA determination. Section 3 illustrates the application of the proposed procedure to two relevant case studies. Then, Section 4 discusses the results, and Section 5 draws the conclusions.

[1] It is worth stressing that, in the literature, the EAK theorem is referred to with a number of different names such as "Three-axes theorem", "Spatial Aronhold-Kennedy theorem", "Dual of the Aronhold-Kennedy theorem", "3D Kennedy theorem", etc.

2. Materials and methods

In a set of m rigid bodies (links), the relative motions between link pairs[2] are $m\times(m-1)/2$ and the instantaneous screw axes, ISA_{ji} ($\equiv ISA_{ij}$) with $j,i\in\{1,\ldots,m|\ (j\neq i)\&(j>i)\}$, that identify their instantaneous status are as many. Nevertheless, if (m–1) of such relative motions are known, the remaining ones can be determined by means of the relative motion theorems [26], that is, at most (m–1) relative motions are independent in the worst case, which is the one where the m links are not connected through kinematic pairs/chains.[3]

Hereafter, with reference to the motion of link j with respect to link i (Fig. 1), the ISA_{ji} will be geometrically identified by the ordered couple (A_{ji}, $\mathbf{u}_{ji}$) where A_{ji} is a point belonging to ISA_{ji} and $\mathbf{u}_{ji}$ is a unit vector parallel to ISA_{ji}; the angular velocity, $\boldsymbol{\omega}_{ji}$, will be put equal to $\omega_{ji}\mathbf{u}_{ji}$ and will be assigned through its signed magnitude ω_{ji}. In addition, if $\omega_{ji}\neq 0$ (i.e., the relative motion is a helical motion), the velocity,[4] ${}^{i}\mathbf{v}_{A_{ji}|j}$, of point A_{ji} ($\in ISA_{ji}$) will be put equal to $\omega_{ji}p_{ji}\mathbf{u}_{ji}$ and assigned through the pitch p_{ji} of the helical motion; otherwise (i.e., if $\omega_{ji}=0$), it will be put equal to $\nu_{ji}\boldsymbol{\tau}_{ji}$ where ν_{ji} is the signed magnitude of the translation velocity and $\boldsymbol{\tau}_{ji}$ is the unit vector that gives the positive direction of translation.[5]

With these notations, the following relationships hold:

(a) if $\omega_{ji}\neq 0$, then $A_{ji}=A_{ij}$, $\mathbf{u}_{ji}=\mathbf{u}_{ij}$, $p_{ji}=p_{ij}$ and $\omega_{ji}=-\omega_{ij}$;
(b) if $\omega_{ji}=0$, then $\boldsymbol{\tau}_{ji}=\boldsymbol{\tau}_{ij}$ and $\nu_{ji}=-\nu_{ij}$.

Moreover, the instantaneous relative motion between links j and i is fully defined when, in the case $\omega_{ji}\neq 0$, ISA_{ji} (i.e., the ordered couple (A_{ji}, $\mathbf{u}_{ji}$)), p_{ji} and ω_{ji} or, in the case $\omega_{ji}=0$, ν_{ji} and $\boldsymbol{\tau}_{ji}$ are known.

2.1. The extended Aronhold-Kennedy theorem and its implications

In a system of three bodies, say links i, j, and k (Fig. 2), the possible relative motions are 3 ($=3\times(3-1)/2$) and the corresponding ISAs are ISA_{ji}, ISA_{jk} and ISA_{ik}, but, when only 2 ($=(3-1)$) of such motions are known, the remaining third is uniquely determined. For this system, the extended Aronhold-Kennedy (EAK) theorem states that:

Statement 1. *(EAK theorem)*: "In a system of three bodies the three ISAs of the three possible relative motions share a common normal."

A mnemonic rule to check the applicability of the EAK theorem is the following one:

Rule 1. "The EAK theorem is applicable to two known ISAs if the indices reported in the right subscript of the two known ISAs share a common link-index."[6]

In the system of three bodies shown in Fig. 2, if the two instantaneous relative motions ji and ik[7] are known, the remaining third, that is, the motion jk, is uniquely determined through the relative motion theorems [26]. In addition, since two lines always share a common normal, which is unique if the two lines are skew, the determination of the jk motion through the relative motion theorem and the known data of the ji and ik motions is able to check the correctness of the EAK theorem and to provide the analytic relationships that relates the three motions. This determination is illustrated below together with a corollary that immediately follows.

The two known motions ji and ik may only be[8]

1st case (Hel-Hel): two helical motions (Fig. 3(a)), which, with our notations, are assigned by giving (A_{ji}, $\mathbf{u}_{ji}$) (i.e., the ISA_{ji}), p_{ji}, and ω_{ji} for the ji motion and (A_{ik}, $\mathbf{u}_{ik}$) (i.e., the ISA_{ik}), p_{ik}, and ω_{ik} for the ik motion;

2nd case (Hel-Tra): one helical motion and one translational motion (Fig. 3(b)), which, with our notations, if the ji motion is the helical one, are assigned by giving (A_{ji}, $\mathbf{u}_{ji}$) (i.e., the ISA_{ji}), p_{ji}, and ω_{ji} for the ji motion and ν_{ik} and $\boldsymbol{\tau}_{ik}$ for the ik motion;

3rd case (Tra-Tra): two translational motions, which, with our notations, are assigned by giving ν_{ji} and $\boldsymbol{\tau}_{ji}$ for the ji motion and ν_{ik} and $\boldsymbol{\tau}_{ik}$ for the ik motion.

In the Tra-Tra case, the EAK theorem demonstration is trivial. Indeed, the relative motion theorems immediately bring one to conclude that the third unknown motion (i.e., the jk motion) must be a translation with translation velocity $\nu_{jk}\tau_{jk}=\nu_{ji}\tau_{ji}+\nu_{ik}\tau_{ik}$, which

[2] Here, for a generic link pair constituted by links i and j, the motion of link i with respect to link j and its inverse motion (i.e., the motion of link j with respect to link i) are considered the same relative motion since the velocity fields associated to the two motions are immediately obtained from one another through a change of sign.

[3] It is worth stressing that, if the m links are connected to form a particular mechanism with f degrees of freedom, the number of independent relative motions is the minimum value between (m–1) and f.

[4] Hereafter, ${}^{i}\mathbf{v}_{P|j}$ will denote the velocity of point P when the point is fixed to link j and the velocity is measured from link i.

[5] In the case of a translation, the ISA_{ji} is the line at infinity (ideal line) that is the geometric locus of the points at infinity of the planes perpendicular to the translation direction.

[6] It is worth stressing that, if rule 1 is respected, the elimination of the common link-index leaves the couple of link-indices of the third ISA that must be perpendicular to the common normal of the two known ISAs.

[7] Hereafter, for the sake of brevity, the phrase "motion mn" will be used to mean "instantaneous relative motion of link m with respect to link n"

[8] Here, a pure rotation is considered a particular case of helical motion since it is sufficient to put the pitch equal to zero in the formulas deduced for a helical motion to obtain the formulas valid for a pure rotation.

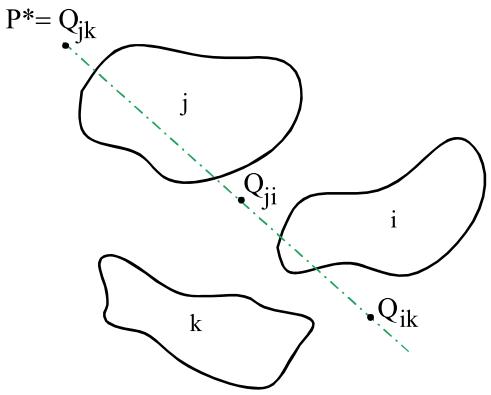

Fig. 2. System of three bodies, denoted i, j, and k: the dash-dot line is the common normal shared by ISA_{ik}, ISA_{ji}, and ISA_{jk}, the EAK theorem refers to, and points Q_{ik}, Q_{ji}, and Q_{jk} are the intersection of this line with ISA_{ik}, ISA_{ji}, and ISA_{jk}, respectively.

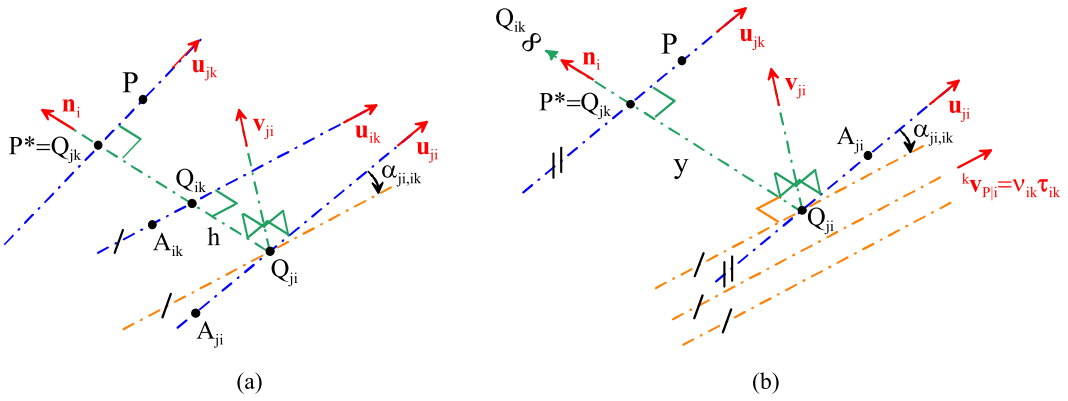

Fig. 3. EAK theorem: (a) both the ji and ik motions are helical motions, (b) the ji motion is a helical motion and the ik motion is a translational motion.

is parallel to the plane the two known translation velocities (i.e., $v_{ji}\tau_{ji}$ and $v_{ik}\tau_{ik}$) lie on thus proving the EAK theorem.[9]

In the Hel-Hel case (Fig. 3(a)), the relative motion theorems yield

$$ {}^{k}\mathbf{v}_{P|j} = {}^{i}\mathbf{v}_{P|j} + {}^{k}\mathbf{v}_{P|i} \tag{1a} $$

$$ \omega_{jk}\mathbf{u}_{jk} = \omega_{ji}\mathbf{u}_{ji} + \omega_{ik}\mathbf{u}_{ik} \tag{1b} $$

Eq. (1b) allows the computation of ω_{jk} and $\mathbf{u}_{jk}$ as functions of the data with the following explicit formulas (remind that $\omega_{ki} = -\omega_{ik}$)

$$ \mathbf{u}_{jk} = \frac{\omega_{ji}\mathbf{u}_{ji} + \omega_{ik}\mathbf{u}_{ik}}{\| \omega_{ji}\mathbf{u}_{ji} + \omega_{ik}\mathbf{u}_{ik} \|} \tag{2a} $$

$$ \omega_{jk} = \omega_{ji}\left(\mathbf{u}_{ji}\cdot\mathbf{u}_{jk}\right) + \omega_{ik}\left(\mathbf{u}_{ik}\cdot\mathbf{u}_{jk}\right) \tag{2b} $$

$$ \frac{\omega_{ji}}{\omega_{ki}} = \frac{\mathbf{u}_{ik}\cdot\left(\mathbf{n}_i\times\mathbf{u}_{jk}\right)}{\mathbf{u}_{ji}\cdot\left(\mathbf{n}_i\times\mathbf{u}_{jk}\right)} = \frac{\mathbf{n}_i\cdot\left(\mathbf{u}_{ik}\times\mathbf{u}_{jk}\right)}{\mathbf{n}_i\cdot\left(\mathbf{u}_{ji}\times\mathbf{u}_{jk}\right)} \tag{2c} $$

where $\mathbf{n}_i \equiv (\mathbf{u}_{ji}\times\mathbf{u}_{ik})/\| \mathbf{u}_{ji}\times\mathbf{u}_{ik} \|$ is the unit vector of the common normal to ISA_{ji} and ISA_{ik}. Eq. (2a) shows that ISA_{jk} must lie on a plane perpendicular to $\mathbf{n}_i$; whereas, Eq. (2c) highlights that the VC (ω_{ji}/ω_{ki}), which is the ratio of the two known signed-magnitudes of angular velocities, depends only on the directions of the three ISAs.

[9] It is worth noting that, in this case, three planes perpendicular to the three translation velocities that share a common point must also share a line, which is the common normal, shared by the three ideal lines, that play the role of ISAs in the Tra-Tra case.

Moreover, if point[10] P of Eq. (1a) is a generic point of the unknown ISA_{jk} and Q_{ji} (Q_{ik}) is the intersection point of the known ISA_{ji} (ISA_{ik}) with the common normal of ISA_{ji} and ISA_{ik}, the following relationships hold

$$ {}^{i}\mathbf{v}_{P|j} = \omega_{ji}\left[p_{ji}\mathbf{u}_{ji} + \left(Q_{ji} - P\right) \times \mathbf{u}_{ji}\right];\ {}^{k}\mathbf{v}_{P|i} = \omega_{ik}\left[p_{ik}\mathbf{u}_{ik} + (Q_{ik} - P) \times \mathbf{u}_{ik}\right];\ {}^{k}\mathbf{v}_{P|j} = p_{jk}\omega_{jk}\mathbf{u}_{jk} \tag{3} $$

and the introduction of Eqs. (1b) and (3) into Eq. (1a) transforms Eq. (1a) as follows:

$$ p_{jk}\left(\omega_{ji}\mathbf{u}_{ji} + \omega_{ik}\mathbf{u}_{ik}\right) = \omega_{ji}\left[p_{ji}\mathbf{u}_{ji} + \left(Q_{ji} - P\right) \times \mathbf{u}_{ji}\right] + \omega_{ik}\left[p_{ik}\mathbf{u}_{ik} + (Q_{ik} - P) \times \mathbf{u}_{ik}\right] \tag{4} $$

where the coordinates of points Q_{ji} and Q_{ik} can be computed as reported in Appendix A (see formulas (A.4)); whereas p_{jk} and the coordinates of point P are unknowns.

Since point P is any point of ISA_{jk}, if, without losing generality, point P is assumed coincident with the intersection, P* (see Fig. 3 (a)), of ISA_{jk} with the plane, (Q_{ji}, $\mathbf{u}_{ji}$, $\mathbf{n}_i$), passing through point Q_{ji} and parallel to the mutually orthogonal unit vectors $\mathbf{u}_{ji}$ and $\mathbf{n}_i$, the following relationships can be written

$$ \begin{cases} \left(P - Q_{ji}\right) \equiv \left(P^{*} - Q_{ji}\right) = x\mathbf{u}_{ji} + y\mathbf{n}_i \\ \left(P - Q_{ik}\right) \equiv \left(P^{*} - Q_{ik}\right) = x\mathbf{u}_{ji} + (y - h)\mathbf{n}_i \end{cases} \tag{5} $$

where x and y are two scalar unknowns that locate point P* on the plane (Q_{ji}, $\mathbf{u}_{ji}$, $\mathbf{n}_i$). The introduction of formulas (5) into Eq. (4) gives the following system of three equations in three unknowns (i.e., p_{jk}, x, and y):

$$ x \parallel \mathbf{u}_{ji} \times \mathbf{u}_{ik} \parallel \mathbf{n}_i + y\left(\mathbf{n}_i \times \mathbf{a}_i\right) + p_{jk}\mathbf{a}_i = \mathbf{b}_i \tag{6} $$

with

$$ \mathbf{a}_i \equiv \mathbf{u}_{ik} - \left(\frac{\omega_{ji}}{\omega_{ki}}\right)\mathbf{u}_{ji};\ \mathbf{b}_i \equiv p_{ik}\mathbf{u}_{ik} - \left(\frac{\omega_{ji}}{\omega_{ki}}\right)p_{ji}\mathbf{u}_{ji} + h(\mathbf{n}_i \times \mathbf{u}_{ik}) \tag{7} $$

The dot products of Eq. (6) by $\mathbf{n}_i$, by $\mathbf{a}_i$, and by ($\mathbf{n}_i \times \mathbf{a}_i$), after some rearrangement, yield the following explicit expressions of the unknowns:

$$ x = 0 \tag{8a} $$

$$ p_{jk} = \frac{p_{ik} - \left(\frac{\omega_{ji}}{\omega_{ki}}\right)\left[\left(p_{ji} + p_{ik}\right)\left(\mathbf{u}_{ji} \cdot \mathbf{u}_{ik}\right) - h \parallel \mathbf{u}_{ji} \times \mathbf{u}_{ik} \parallel\right] + \left(\frac{\omega_{ji}}{\omega_{ki}}\right)^2 p_{ji}}{1 - 2\left(\frac{\omega_{ji}}{\omega_{ki}}\right)\left(\mathbf{u}_{ji} \cdot \mathbf{u}_{ik}\right) + \left(\frac{\omega_{ji}}{\omega_{ki}}\right)^2} = \frac{p_{ik} - \left(\frac{\omega_{ji}}{\omega_{ki}}\right)\left[\left(p_{ji} + p_{ik}\right)\cos\alpha_{ji,ik} - h\sin\alpha_{ji,ik}\right] + \left(\frac{\omega_{ji}}{\omega_{ki}}\right)^2 p_{ji}}{1 - 2\left(\frac{\omega_{ji}}{\omega_{ki}}\right)\cos\alpha_{ji,ik} + \left(\frac{\omega_{ji}}{\omega_{ki}}\right)^2} \tag{8b} $$

$$ y = \frac{\left(\frac{\omega_{ji}}{\omega_{ki}}\right)\left(p_{ji} - p_{ik}\right) \parallel \mathbf{u}_{ji} \times \mathbf{u}_{ik} \parallel + h\left[1 - \left(\frac{\omega_{ji}}{\omega_{ki}}\right)\left(\mathbf{u}_{ji} \cdot \mathbf{u}_{ik}\right)\right]}{1 - 2\left(\frac{\omega_{ji}}{\omega_{ki}}\right)\left(\mathbf{u}_{ji} \cdot \mathbf{u}_{ik}\right) + \left(\frac{\omega_{ji}}{\omega_{ki}}\right)^2} = \frac{\left(\frac{\omega_{ji}}{\omega_{ki}}\right)\left(p_{ji} - p_{ik}\right)\sin\alpha_{ji,ik} + h\left[1 - \left(\frac{\omega_{ji}}{\omega_{ki}}\right)\cos\alpha_{ji,ik}\right]}{1 - 2\left(\frac{\omega_{ji}}{\omega_{ki}}\right)\cos\alpha_{ji,ik} + \left(\frac{\omega_{ji}}{\omega_{ki}}\right)^2} \tag{8c} $$

where the relationships (see Fig. 3(a)) $\cos\alpha_{ji,ik} = \mathbf{u}_{ji} \cdot \mathbf{u}_{ik}$ and $\sin\alpha_{ji,ik} = \parallel \mathbf{u}_{ji} \times \mathbf{u}_{ik} \parallel$ have been used to deduce the last expressions of Eqs. (8b) and (8c). Eqs. (2a) and (8a) prove that ISA_{jk} must be perpendicular to $\mathbf{n}_i$ and must intersect the line (Q_{ji}, $\mathbf{n}_i$), that is, they prove the EAK theorem in the Hel-Hel case. After having demonstrated that $\mathbf{n}_i$ is perpendicular to the three unit vectors $\mathbf{u}_{ji}$, $\mathbf{u}_{ik}$, and $\mathbf{u}_{jk}$, the VC expression given by formula (2c) can be completed and geometrically interpreted as follows:

$$ \frac{\omega_{ji}}{\omega_{ki}} = \frac{\mathbf{u}_{ik} \cdot \left(\mathbf{n}_i \times \mathbf{u}_{jk}\right)}{\mathbf{u}_{ji} \cdot \left(\mathbf{n}_i \times \mathbf{u}_{jk}\right)} = \frac{\mathbf{n}_i \cdot \left(\mathbf{u}_{ik} \times \mathbf{u}_{jk}\right)}{\mathbf{n}_i \cdot \left(\mathbf{u}_{ji} \times \mathbf{u}_{jk}\right)} = \frac{\sin\alpha_{ik,jk}}{\sin\alpha_{ji,jk}} \tag{9} $$

where $\alpha_{ji,jk}$ ($\alpha_{ik,jk}$) is the oriented angle, counterclockwise with respect to $\mathbf{n}_i$, that goes from $\mathbf{u}_{ji}$ ($\mathbf{u}_{ik}$) to $\mathbf{u}_{jk}$. Hereafter, the notation $\alpha_{qr,qt}$ (see Fig. 3(a)) will denote the oriented angle, counterclockwise with respect to $\mathbf{n}_q$, that goes from $\mathbf{u}_{qr}$ (i.e., ISA_{qr}) to $\mathbf{u}_{qt}$ (i.e., ISA_{qt}) where $\mathbf{n}_q$ is the unit vector of the common normal to ISA_{qr}, ISA_{qt}, and ISA_{rt}.

In the Hel-Tra case (Fig. 3(a)), the relative motion theorems (see Eqs. (1)) yield ($\omega_{ik} = 0;\ {}^{k}\mathbf{v}_{P|i} = v_{ik}\tau_{ik}$)

$$ {}^{k}\mathbf{v}_{P|j} = {}^{i}\mathbf{v}_{P|j} + v_{ik}\tau_{ik} \tag{10a} $$

$$ \omega_{jk}\mathbf{u}_{jk} = \omega_{ji}\mathbf{u}_{ji} \Rightarrow \begin{cases} \omega_{jk} = \omega_{ji} \\ \mathbf{u}_{jk} = \mathbf{u}_{ji} \end{cases} \tag{10b} $$

Eq. (10b) shows that, in this case, there are two parallel ISAs (i.e., ISA_{ji} and ISA_{jk}); as a consequence, the common normal is not

[10] Hereafter, for a point, a capital letter in plain text (e.g., P) refers to the point as a geometric entity; whereas, the same capital letter in italic (e.g., *P*) refers to the position vector that locates the point in a fixed reference system.

uniquely determined. Nevertheless, its direction, given through the unit vector $\mathbf{n}_i$, is uniquely determined since the common normal to ISA_{ji} and ISA_{ik}, which, in this case, is the line at infinity of the planes perpendicular to $\boldsymbol{\tau}_{ik}$ (i.e., to the translation direction) must be an intersection between one of the planes perpendicular to $\boldsymbol{\tau}_{ik}$ and one of the planes perpendicular to $\mathbf{u}_{ji}$ (i.e., to ISA_{ji}), that is, the following relationship holds:

$$\mathbf{n}_i = \frac{\mathbf{u}_{ji} \times \tau_{ik}}{\| \mathbf{u}_{ji} \times \tau_{ik} \|} \tag{11}$$

If point P of Eq. (10a) is a generic point of the unknown ISA_{jk} and Q_{ji} is a point of the known ISA_{ji} the following relationships hold

$${}^{i}\mathbf{v}_{P|j} = \omega_{ji}\left[p_{ji}\mathbf{u}_{ji} + \left(Q_{ji} - P\right) \times \mathbf{u}_{ji}\right];\ {}^{k}\mathbf{v}_{P|j} = p_{jk}\omega_{jk}\mathbf{u}_{jk} \tag{12}$$

and the introduction of Eqs. (10b) and (12) into Eq. (10a) transforms Eq. (10a) as follows:

$$p_{jk}\omega_{ji}\mathbf{u}_{ji} = \omega_{ji}\left[p_{ji}\mathbf{u}_{ji} + \left(Q_{ji} - P\right) \times \mathbf{u}_{ji}\right] + v_{ik}\tau_{ik} \tag{13}$$

where p_{jk} and the coordinates of point P are unknowns.

Since point P is any point of ISA_{jk}, if, without losing generality, point P is assumed coincident with the intersection, P* (see Fig. 3 (b)), of ISA_{jk} with the plane, (Q_{ji}, $\mathbf{n}_i$, $\mathbf{u}_{ji}\times\mathbf{n}_i$), passing through point Q_{ji} and parallel to the mutually orthogonal unit vectors $\mathbf{n}_i$ and $\mathbf{u}_{ji}\times\mathbf{n}_i$, the following relationships can be written

$$\left(P - Q_{ji}\right) \equiv \left(P^* - Q_{ji}\right) = y\mathbf{n}_i + z\left(\mathbf{u}_{ji} \times \mathbf{n}_i\right) \tag{14}$$

where y and z are two scalar unknowns that locate point P* on the plane (Q_{ji}, $\mathbf{n}_i$, $\mathbf{u}_{ji}\times\mathbf{n}_i$). The introduction of formula (14) into Eq. (13) gives the following system of three equations in three unknowns (i.e., p_{jk}, y, and z):

$$p_{jk}\mathbf{u}_{ji} + y\left(\mathbf{n}_i \times \mathbf{u}_{ji}\right) + z\,\mathbf{n}_i = p_{ji}\mathbf{u}_{ji} + \frac{v_{ik}}{\omega_{ji}}\tau_{ik} \tag{15}$$

Eventually, the dot products of Eq. (15) by $\mathbf{n}_i$, by $\mathbf{u}_{ji}$ and by $\mathbf{u}_{ji}\times\mathbf{n}_i$ yield the following explicit expressions of the unknowns as functions of the data:

$$z = 0 \tag{16a}$$

$$p_{jk} = p_{ji} + \frac{v_{ik}}{\omega_{ji}}\left(\tau_{ik} \cdot \mathbf{u}_{ji}\right) \tag{16b}$$

$$y = \frac{v_{ik}}{\omega_{ji}}\tau_{ik} \cdot \left(\mathbf{n}_i \times \mathbf{u}_{ji}\right) \tag{16c}$$

Eqs. (16a) and (10b) highlight that the ISA_{jk} must intersect (see Eq. (16a)) the line (Q_{ji}, $\mathbf{n}_i$) and be perpendicular (see Eq. (10b)) to the same line, which plays the role of common normal to the three ISAs. Such a result proves the EAK theorem in the Hel-Tra case.

Eq. (16c) can be rewritten (see Eq. (11) and Fig. 3(b)) as follows ($v_{ik} = -v_{ki}$):

$$\frac{v_{ki}}{\omega_{ji}} = \frac{\left(A_{jk} - A_{ji}\right) \cdot \left(\mathbf{u}_{ji} \times \tau_{ik}\right)}{\tau_{ik} \cdot \left[\mathbf{u}_{ji} \times \left(\mathbf{u}_{ji} \times \tau_{ik}\right)\right]} = \frac{\left(A_{jk} - A_{ji}\right) \cdot \left(\mathbf{u}_{ji} \times \tau_{ik}\right)}{\left(\mathbf{u}_{ji} \cdot \tau_{ik}\right)^2 - 1} = -\frac{\left(A_{jk} - A_{ji}\right) \cdot \left(\mathbf{u}_{ji} \times \tau_{ik}\right)}{\sin^2\alpha_{ji,ik}} \tag{17}$$

where the relationship $\mathbf{u}_{ji} \times (\mathbf{u}_{ji} \times \tau_{ik}) = (\mathbf{u}_{ji} \cdot \tau_{ik})\mathbf{u}_{ji} - \tau_{ik} \Rightarrow \tau_{ik} \cdot [\mathbf{u}_{ji} \times (\mathbf{u}_{ji} \times \tau_{ik})] = (\mathbf{u}_{ji} \cdot \tau_{ik})^2 - 1 = -\sin^2\alpha_{ji,ik}$ has been considered. Eq. (17) shows that the explicit expression of the VC (v_{ki}/ω_{ji}), (i.e., the ratio of the two known signed-magnitudes of the translation and angular velocities) depends only on the geometric data that identifies the three ISAs (i.e., (A_{ji}, $\mathbf{u}_{ji}$), (A_{jk}, $\mathbf{u}_{jk}$=$\mathbf{u}_{ji}$), and $\boldsymbol{\tau}_{ik}$) even in the case that one ISA is an ideal line. Moreover, if Eq. (17) was applied to the three links i, j, and r with r≠k, where the relative motion ir is a translation with translation velocity ${}^{r}\mathbf{v}_{P|i} = v_{ir}\tau_{ir}$, it would yield the expression of the VC (v_{ri}/ω_{ji}) that differs from the one of the VC (v_{ki}/ω_{ji}) (i.e., Eq. (17)) only for the replacement of k with r; thus, the ratio (v_{ki}/ω_{ji})/(v_{ri}/ω_{ji}), which is equal to the new VC (v_{ki}/v_{ri}), is

$$\frac{v_{ki}}{v_{ri}} = \frac{\left(A_{jk} - A_{ji}\right) \cdot \left(\mathbf{u}_{ji} \times \tau_{ik}\right)\left[\left(\mathbf{u}_{ji} \cdot \tau_{ir}\right)^2 - 1\right]}{\left(A_{jr} - A_{ji}\right) \cdot \left(\mathbf{u}_{ji} \times \tau_{ir}\right)\left[\left(\mathbf{u}_{ji} \cdot \tau_{ik}\right)^2 - 1\right]} = \frac{\left(A_{jk} - A_{ji}\right) \cdot \left(\mathbf{u}_{ji} \times \tau_{ik}\right)\sin^2\alpha_{ji,ir}}{\left(A_{jr} - A_{ji}\right) \cdot \left(\mathbf{u}_{ji} \times \tau_{ir}\right)\sin^2\alpha_{ji,ik}} \tag{18}$$

which is the explicit expression of the VC that relates the signed magnitudes of two relative translations in a set of four links (i.e., links i, j, k, and r). It is worth noting that, since link j can be any link, choosing link j so that ISA_{ji} (i.e., (A_{ji}, $\mathbf{u}_{ji}$)) is neither parallel to $\boldsymbol{\tau}_{ik}$ nor parallel to $\boldsymbol{\tau}_{ir}$ is always possible.

The EAK theorem allows the demonstration of the following corollary:

Statement 2. *(four-axes (FA) theorem)*: "Let i, j, k, and r be four bodies, if the ISAs of the jk, ik, jr, and ir relative motions are four distinct and known lines, then the ISA of the ji (kr) relative motion is the common normal to the following two lines: (i) the common normal to ISA_{jk} and ISA_{ik} (to ISA_{jk} and ISA_{jr}), and (ii) the common normal to ISA_{jr} and ISA_{ir} (to ISA_{ik} and ISA_{ir})."

Proof. Applying the EAK theorem to the three bodies i, j, and k (j, k, and r) brings one to conclude that ISA_{ji} (ISA_{kr}) must be perpendicular to the common normal to ISA_{jk} and ISA_{ik} (to ISA_{jk} and ISA_{jr}), and applying the EAK theorem to the three bodies i, j, and r (i, k, and r) brings one to conclude that ISA_{ji} (ISA_{kr}) must also be perpendicular to the common normal to ISA_{jr} and ISA_{ir} (to ISA_{ik} and ISA_{ir}). *Q.E.D.*

A mnemonic rule to check the applicability of the FA theorem is the following one:

Rule 2. "The FA theorem is applicable to four known ISAs if the indices reported in the right subscript of the four known ISAs (i.e., {jk, ik, jr, ir}) can be grouped into two pairs that share one link-index whose elimination leaves the same couple of link-indices in both the pairs no matter how they are ordered."

From an analytic point of view, the FA theorem can be exploited as follows. Fig. 4 shows the four known ISAs and the geometric determination of ISA_{ji}. With reference to Fig. 4, the following relationships hold:

$$\mathbf{n}_k = \frac{\mathbf{u}_{jk} \times \mathbf{u}_{ik}}{\| \mathbf{u}_{jk} \times \mathbf{u}_{ik} \|}; \; \mathbf{n}_r = \frac{\mathbf{u}_{jr} \times \mathbf{u}_{ir}}{\| \mathbf{u}_{jr} \times \mathbf{u}_{ir} \|}; \tag{19a}$$

$$Q_{ji} = Q_{jk} + y_{Q_{ji}} \mathbf{n}_k; \; Q'_{ji} = Q_{jr} + y_{Q'_{ji}} \mathbf{n}_r; \tag{19b}$$

$$\mathbf{u}_{ji} = \frac{\mathbf{n}_r \times \mathbf{n}_k}{\| \mathbf{n}_r \times \mathbf{n}_k \|}; \; \left(Q_{ji} - Q'_{ji} \right) = h_{ji} \mathbf{u}_{ji}; \tag{19c}$$

where h_{ji}, $y_{Q_{ji}}$, and $y_{Q'_{ji}}$ are three scalar unknowns that must be determined; whereas, Q_{jk} (Q_{jr}) has been determined by using the formulas reported in Appendix A with the data that locate ISA_{jk} and ISA_{ik} (ISA_{jr} and ISA_{ir}), that is, (A_{jk}, $\mathbf{u}_{jk}$) and (A_{ik}, $\mathbf{u}_{ik}$) (that is, (A_{jr}, $\mathbf{u}_{jr}$) and (A_{ir}, $\mathbf{u}_{ir}$)). The introduction of formulas (19b) into the second Eq. (19c) yields the following system of three equations in three unknowns (i.e., h_{ji}, $y_{Q_{ji}}$, and $y_{Q'_{ji}}$):

$$y_{Q_{ji}} \mathbf{n}_k - y_{Q'_{ji}} \mathbf{n}_r - h_{ji} \frac{\mathbf{n}_r \times \mathbf{n}_k}{\| \mathbf{n}_r \times \mathbf{n}_k \|} = \left(Q_{jr} - Q_{jk} \right) \tag{20}$$

whose solution gives the following explicit expressions of the three unknowns

$$\begin{cases} h_{ji} = -\left(Q_{jr} - Q_{jk} \right) \cdot \dfrac{\mathbf{n}_r \times \mathbf{n}_k}{\| \mathbf{n}_r \times \mathbf{n}_k \|} \\ y_{Q_{ji}} = \dfrac{\left(Q_{jr} - Q_{jk} \right) \cdot \left[\mathbf{n}_r \times \left(\mathbf{n}_r \times \mathbf{n}_k \right) \right]}{\mathbf{n}_k \cdot \left[\mathbf{n}_r \times \left(\mathbf{n}_r \times \mathbf{n}_k \right) \right]} \\ y_{Q'_{ji}} = -\dfrac{\left(Q_{jr} - Q_{jk} \right) \cdot \left[\mathbf{n}_k \times \left(\mathbf{n}_r \times \mathbf{n}_k \right) \right]}{\mathbf{n}_r \cdot \left[\mathbf{n}_k \times \left(\mathbf{n}_r \times \mathbf{n}_k \right) \right]} \end{cases} \tag{21}$$

The above geometric/analytic discussion refers to the case in which $\mathbf{n}_k \neq \pm \mathbf{n}_r$ (i.e., the two lines (Q_{jk}, $\mathbf{n}_k$) and (Q_{jr}, $\mathbf{n}_r$) are skew) and the two lines (Q_{jk}, $\mathbf{n}_k$) and (Q_{jr}, $\mathbf{n}_r$) are uniquely determined from the four known ISAs (i.e., from (A_{jk}, $\mathbf{u}_{jk}$), (A_{ik}, $\mathbf{u}_{ik}$), (A_{jr}, $\mathbf{u}_{jr}$) and (A_{ir}, $\mathbf{u}_{ir}$)). The discussion of the remaining possible cases follows.

With reference to the system of the four links i, j, k and r (i.e. the one the FA theorem refers to), the relative motion theorem bring one to write (see Fig. 4 for the notations)

$$\left. \begin{aligned} \omega_{ji} \mathbf{u}_{ji} &= \omega_{jk} \mathbf{u}_{jk} + \omega_{ki} \mathbf{u}_{ik} \\ \omega_{ji} \mathbf{u}_{ji} &= \omega_{jr} \mathbf{u}_{jr} + \omega_{ri} \mathbf{u}_{ir} \end{aligned} \right\} \Rightarrow \omega_{ji} \mathbf{u}_{ji} = \omega_{jk} \mathbf{u}_{jk} + \omega_{ki} \mathbf{u}_{ik} = \omega_{jr} \mathbf{u}_{jr} + \omega_{ri} \mathbf{u}_{ir} \tag{22a}$$

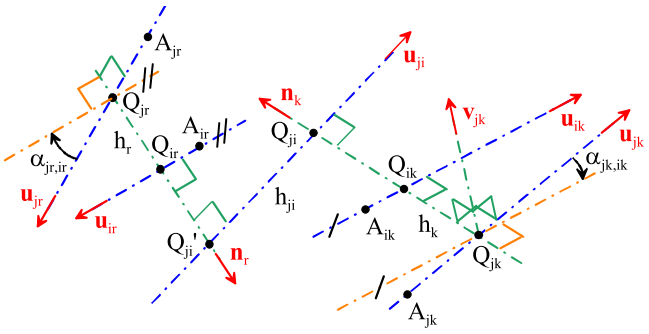

Fig. 4. Determination of ISA_{ji} through the FA theorem in the case of skew lines.

$$\left.\begin{array}{l} {}^{i}\mathbf{v}_{Q_{ji}|j} = {}^{k}\mathbf{v}_{Q_{ji}|j} + {}^{i}\mathbf{v}_{Q_{ji}|k} \\ {}^{i}\mathbf{v}_{Q_{ji}|j} = {}^{i}\mathbf{v}_{Q_{ji}'|j} = {}^{r}\mathbf{v}_{Q_{ji}'|j} + {}^{i}\mathbf{v}_{Q_{ji}'|r} \end{array}\right\} \Rightarrow \left[\begin{array}{l} p_{ji}\omega_{ji}\mathbf{u}_{ji} = \omega_{jk}\left(p_{jk}\mathbf{u}_{jk} - y_{Q_{ji}}\mathbf{n}_k \times \mathbf{u}_{jk}\right) + \omega_{ki}\left[p_{ik}\mathbf{u}_{ik} - \left(y_{Q_{ji}} - h_k\right)\mathbf{n}_k \times \mathbf{u}_{ik}\right] = \\ = \omega_{jr}\left(p_{jr}\mathbf{u}_{jr} - y_{Q_{ji}'}\mathbf{n}_r \times \mathbf{u}_{jr}\right) + \omega_{ri}\left[p_{ir}\mathbf{u}_{ir} - \left(y_{Q_{ji}'} - h_r\right)\mathbf{n}_r \times \mathbf{u}_{ir}\right] \end{array}\right. \tag{22b}$$

The last equality of Eq. (22a) constitutes a linear system of three equations that are linearly independent and compatible if and only if the four unit vectors $\mathbf{u}_{jk}$, $\mathbf{u}_{ik}$, $\mathbf{u}_{jr}$, and $\mathbf{u}_{ir}$ are not coplanar (i.e., if the case shown in Fig. 4 occurs). In this case, if one out of the four signed magnitudes ω_{jk}, ω_{ik}, ω_{jr}, and ω_{ir} is assigned the remaining three are uniquely determined and, as a consequence, $\omega_{ji}\mathbf{u}_{ji}$ is determined, too, that is, the instantaneous motion has only one DOF. Differently, if the four unit vectors $\mathbf{u}_{jk}$, $\mathbf{u}_{ik}$, $\mathbf{u}_{jr}$, and $\mathbf{u}_{ir}$ are coplanar with $\mathbf{u}_{jk}$ not parallel to $\mathbf{u}_{ik}$ then (see last equality of Eq. (22a)) also $\mathbf{u}_{jr}$ must not be parallel to $\mathbf{u}_{ir}$ (i.e., the case $\mathbf{n}_k = \pm\mathbf{n}_r$ with the two lines (Q_{jk}, $\mathbf{n}_k$) and (Q_{jr}, $\mathbf{n}_r$) uniquely determined occurs) and the system is singular since it has only two independent equations; therefore, in this second case, the instantaneous motion has two DOF (i.e., two signed magnitudes that share one common index, that is, k or r, must be assigned to determine the remaining ones and $\omega_{ji}\mathbf{u}_{ji}$). Accordingly, in a single-DOF mechanism, such a condition may occur only at a singular configuration of the mechanism.

Moreover, if $\mathbf{u}_{jk}$ is parallel to $\mathbf{u}_{ik}$ and $\mathbf{u}_{jr}$ is parallel to $\mathbf{u}_{ir}$, but $\mathbf{u}_{jk}$ is not parallel to $\mathbf{u}_{jr}$ (i.e., the case $\mathbf{n}_k \neq \pm\mathbf{n}_r$ with the two lines (Q_{jk}, $\mathbf{n}_k$) and (Q_{jr}, $\mathbf{n}_r$) not-uniquely determined occurs) then the last equality of Eq. (22a) will be satisfied if and only if ω_{ji} is equal to 0, that is, if and only if the ji motion is a translation. In this case, Fig. 3(b) and the above-reported analysis of the Hel-Tra case bring one to conclude that the translation direction of the ji motion must be perpendicular both to $\mathbf{n}_k$ and $\mathbf{n}_r$, that is, it must be parallel to $\mathbf{n}_k \times \mathbf{n}_r$, which yields $\tau_{ji} = \mathbf{n}_k \times \mathbf{n}_r / \parallel \mathbf{n}_k \times \mathbf{n}_r \parallel$.

Eventually, if $\mathbf{u}_{jk}$, $\mathbf{u}_{ik}$, $\mathbf{u}_{jr}$, and $\mathbf{u}_{ir}$ are all parallel, the lines (Q_{jk}, $\mathbf{n}_k$) and (Q_{jr}, $\mathbf{n}_r$) are always undetermined. In this case, if the four known and parallel ISAs are arranged so that ISA_{jk} and ISA_{ik} lie on a plane not-parallel to the plane which ISA_{jr} and ISA_{ik} lie on, then $\mathbf{n}_k \neq \pm\mathbf{n}_r$ and ISA_{ji} must be the intersection line between these two not-parallel planes. Otherwise, if the four known and parallel ISAs are arranged so that ISA_{jk} and ISA_{ik} lie on a plane different-from and parallel-to the plane which ISA_{jr} and ISA_{ik} lie on, then $\mathbf{n}_k = \pm\mathbf{n}_r$ and ISA_{ji} must be the line at infinity these two parallel planes shares, that is, the ji relative motion must be a translation with translation direction perpendicular to these two parallel planes, which yields $\tau_{ji} = \mathbf{n}_k \times \mathbf{u}_{jk} / \|\mathbf{n}_k \times \mathbf{u}_{jk}\| \equiv \pm\mathbf{n}_r \times \mathbf{u}_{jr} / \parallel \mathbf{n}_r \times \mathbf{u}_{jr} \parallel$. Finally, if the four known and parallel ISAs are arranged so that they all lie on the same plane, the ISA_{ji} motion is undetermined since this geometric condition shares the properties of both the previously-analyzed two cases (i.e., any line parallel to the ISAs (even the line at infinity) that lies on the plane of the four known ISAs can be seen as an intersection line of two coincident planes) and the resulting instantaneous motion has more than one DOF. Accordingly, in a single-DOF mechanism, this condition may occur only at a singular configuration of the mechanism.

The fact that, out of singular configurations, the ISA_{ji} can always be determined through the FA theorem makes the FA theorem a simple geometric and analytic tool for the direct determination of unknown ISAs (secondary ISAs) in a spatial single-DOF mechanism. As a consequence, the FA theorem provides the spatial counterpart of the rule used to draw segments that connect link indices in circle diagrams [27,28] when secondary ICs must be determined in single-DOF planar mechanisms; thus, it extends the use of circle diagrams (and/or their alternatives) to the ISA determination in spatial single-DOF mechanisms.

2.2. Constraints on the ISAs due to the kinematic pairs

The kinematic pairs that can be encountered in a spatial mechanism are only ten, six of which are lower pairs and the remaining four are higher pairs. The lower pairs are (see Fig. 5): revolute (R) pair, prismatic (P) pair, helical (H) pair, cylindrical (C) pair,

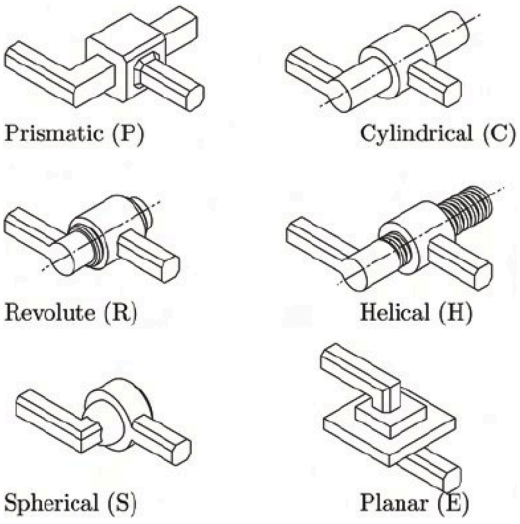

Fig. 5. Lower kinematic pairs (reproduced from Ref. [29]).

spherical (S) pair, and planar (E) pair. The higher pairs are: rolling point-contact (R_P), rolling line-contact (R_L), sliding point-contact (S_P), and sliding line-contact (S_L).

The ji relative motion is uniquely determined when the following data are known: (A_{ji}, $\mathbf{u}_{ji}$) (i.e., the ISA_{ji}), p_{ji}, and ω_{ji}. Such data constitute a set of six scalar parameters since (A_{ji}, $\mathbf{u}_{ji}$) contains only four independent parameters (remind that A_{ji} is any point of the line and $\mathbf{u}_{ji}$ is a unit vector). If links j and i are connected through one of the ten possible kinematic pairs, a number of these parameters, which is equal to (6–f) where f is the DOF of the connecting pair, are uniquely determined. In particular, the known/unknown data are as follows.

2.2.1. Lower pairs

- *Revolute (R) pair (1 DOF)*: ISA_{ji} (i.e., (A_{ji}, $\mathbf{u}_{ji}$)) is known since it coincides with the R-pair axis, $p_{ji}=0$, and ω_{ji} is the unknown joint rate;
- *Prismatic (P) pair (1 DOF)*: if $\boldsymbol{\tau}_{ji}$ is the unit vector that gives the (positive) translation direction imposed by the P-pair, then ISA_{ji} is the line at infinity common to all the planes that are perpendicular to $\boldsymbol{\tau}_{ji}$, $p_{ji}=\infty$, and ν_{ji} is the unknown joint rate;
- *Helical (H) pair (1 DOF)*: ISA_{ji} (i.e., (A_{ji}, $\mathbf{u}_{ji}$)) is known since it coincides with the H-pair axis, p_{ji} is a known constant since it is equal to the H-pair pitch, and ω_{ji} is the unknown joint rate;
- *Cylindrical (C) pair (2 DOF)*: ISA_{ji} (i.e., (A_{ji}, $\mathbf{u}_{ji}$)) is known since it coincides with the C-pair axis; whereas p_{ji} and ω_{ji} are both unknown;
- *Spherical (S) pair (3 DOF)*: the S-pair's center is a point of ISA_{ji} (i.e., A_{ji} is known), $\mathbf{u}_{ji}$ is unknown, $p_{ji}=0$, and ω_{ji} is unknown;
- *Planar (E) pair (3 DOF)*: ISA_{ji} 's direction is perpendicular to the motion plane (i.e., $\mathbf{u}_{ji}$ is known), A_{ji} is unknown, $p_{ji}=0$, and ω_{ji} is unknown.

2.2.2. Higher pairs

- *Rolling (R_L) contact with a contact line (1 DOF)*: ISA_{ji} (i.e., (A_{ji}, $\mathbf{u}_{ji}$)) is known since it coincides with the contact line, $p_{ji}=0$, and ω_{ji} is unknown;
- *Rolling (R_P) contact with a contact point (3 DOF)*: the contact point is a point of ISA_{ji} (i.e., A_{ji} is known), $\mathbf{u}_{ji}$ is unknown, $p_{ji}=0$, and ω_{ji} is unknown;

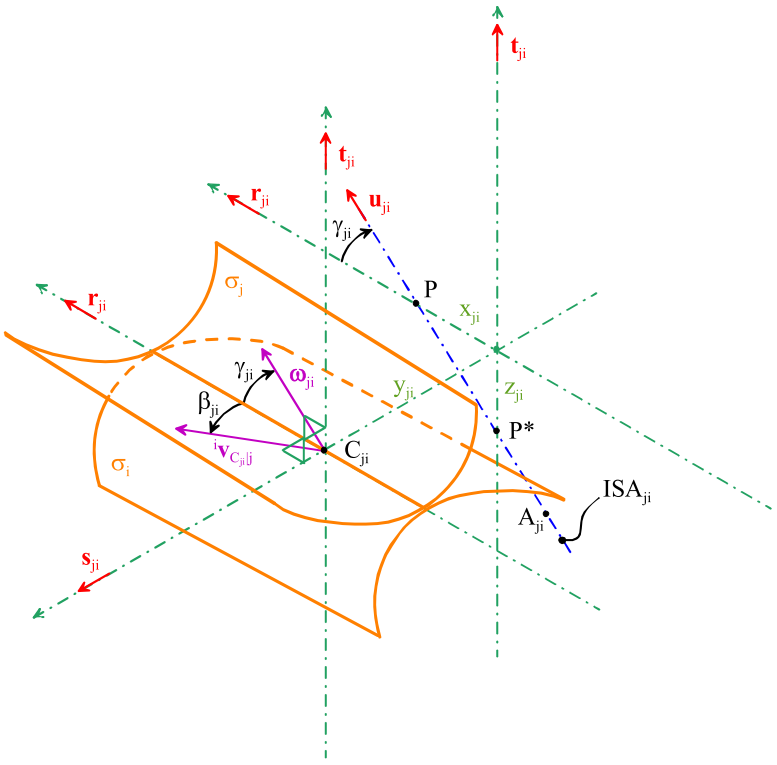

Fig. 6. Sliding contact between links j and i with a contact line (line (C_{ji}, r_{ji})).

– *Sliding (S_L) contact with a contact line (4 DOF) (Fig. 6)*: ISA_{ji} lies on a plane that is parallel to the contact line and is perpendicular to the plane tangent to the two surfaces that touch one another, which implies that A_{ji} is unknown and $\mathbf{u}_{ji}$ has only one unknown component; moreover, p_{ji} and ω_{ji} are related to one another;

For the S_L pair the relationships among the six parameters that identify the ji relative motion can be deduced as follows. With reference to Fig. 6, σ_j and σ_i are the two surfaces fixed to links j and i, respectively, that touch one another along the line (C_{ji}, $\mathbf{r}_{ji}$), which is the contact line; $\mathbf{s}_{ji}$ is the unit vector perpendicular to (C_{ji}, $\mathbf{r}_{ji}$) and lying on the plane tangent both to σ_j and σ_i and $\mathbf{t}_{ji}=\mathbf{r}_{ji}\times\mathbf{s}_{ji}$.

With these notations, (C_{ji}, $\mathbf{r}_{ji}$, $\mathbf{s}_{ji}$), (C_{ji}, $\mathbf{r}_{ji}$, $\mathbf{t}_{ji}$), and (C_{ji}, $\mathbf{s}_{ji}$, $\mathbf{t}_{ji}$) are the tangent plane, the first normal plane, and the second normal plane at the contact line, respectively, of the S_L-pair. The kinematic conditions, imposed by the S_L-pair, are that the sliding velocity ${}^i\mathbf{v}_{C_{ji}|j}$ must lie on the tangent plane (C_{ji}, $\mathbf{r}_{ji}$, $\mathbf{s}_{ji}$) and that the angular velocity $\boldsymbol{\omega}_{ji}$ must lie on the first normal plane (C_{ji}, $\mathbf{r}_{ji}$, $\mathbf{t}_{ji}$). Such conditions yield the following analytic relationships:

$$ {}^i\mathbf{v}_{C_{ji}|j}\cdot\mathbf{t}_{ji}=0\Rightarrow {}^i\mathbf{v}_{C_{ji}|j}={}^iv_{C_{ji}|j}\left(\mathbf{r}_{ji}\cos\beta_{ji}+\mathbf{s}_{ji}\sin\beta_{ji}\right) \tag{23a}$$

$$ \boldsymbol{\omega}_{ji}\cdot\mathbf{s}_{ji}=0\Rightarrow\boldsymbol{\omega}_{ji}=\omega_{ji}\left(\mathbf{r}_{ji}\cos\gamma_{ji}+\mathbf{t}_{ji}\sin\gamma_{ji}\right)=\omega_{ji}\mathbf{u}_{ji}\Rightarrow\mathbf{u}_{ji}=\mathbf{r}_{ji}\cos\gamma_{ji}+\mathbf{t}_{ji}\sin\gamma_{ji} \tag{23b}$$

where γ_{ji} is the angle (i.e., the unique scalar parameter) that fully identifies the unit vector $\mathbf{u}_{ji}$ (i.e., the direction of ISA_{ji}); whereas, ${}^iv_{C_{ji}|j}$ and β_{ji} are the signed magnitude and the angle, respectively, that identify the sliding velocity ${}^i\mathbf{v}_{C_{ji}|j}$ in the tangent plane (C_{ji}, $\mathbf{r}_{ji}$, $\mathbf{s}_{ji}$). Eq. (23b) shows that ISA_{ji} is parallel to the first normal plane (C_{ji}, $\mathbf{r}_{ji}$, $\mathbf{t}_{ji}$). Let point P (P*) be the intersection between ISA_{ji} and the tangent plane (C_{ji}, $\mathbf{r}_{ji}$, $\mathbf{s}_{ji}$) (and the second normal plane (C_{ji}, $\mathbf{s}_{ji}$, $\mathbf{t}_{ji}$)), the following relationships hold:

$$ {}^i\mathbf{v}_{P|j}={}^i\mathbf{v}_{C_{ji}|j}+\omega_{ji}\left(C_{ji}-P\right)\times\mathbf{u}_{ji} \tag{24a}$$

$$ {}^i\mathbf{v}_{P|j}=p_{ji}\omega_{ji}\mathbf{u}_{ji} \tag{24b}$$

$$ \left(P-C_{ji}\right)=x_{ji}\mathbf{r}_{ji}+y_{ji}\mathbf{s}_{ji} \tag{24c}$$

$$ \left.\begin{array}{l}\left(P^*-C_{ji}\right)=y_{ji}\mathbf{s}_{ji}+z_{ji}\mathbf{t}_{ji}\\ \left(P^*-C_{ji}\right)=\left(P-C_{ji}\right)+\mu_{ji}\mathbf{u}_{ji}=\left(x_{ji}+\mu_{ji}\cos\gamma_{ji}\right)\mathbf{r}_{ji}+y_{ji}\mathbf{s}_{ji}+\mathbf{t}_{ji}\mu_{ji}\sin\gamma_{ji}\end{array}\right\}\Rightarrow\left\{\begin{array}{c}\mu_{ji}=-\dfrac{x_{ji}}{\cos\gamma_{ji}}\\ z_{ji}=\mu_{ji}\sin\gamma_{ji}=-x_{ji}\tan\gamma_{ji}\end{array}\right. \tag{24d}$$

where x_{ji} and y_{ji} (y_{ji} and z_{ji}) are two scalar parameters that locate point P (point P*) on the tangent plane (C_{ji}, $\mathbf{r}_{ji}$, $\mathbf{s}_{ji}$) (on the second normal plane (C_{ji}, $\mathbf{s}_{ji}$, $\mathbf{t}_{ji}$)). The introduction of formulas (23a), (24b) and (24c) into Eq. (24a) yields the following system of three equations in the three unknowns p_{ji}, x_{ji} and y_{ji}:

$$ p_{ji}\mathbf{u}_{ji}+x_{ji}\mathbf{r}_{ji}\times\mathbf{u}_{ji}+y_{ji}\mathbf{s}_{ji}\times\mathbf{u}_{ji}=\left(\frac{{}^iv_{C_{ji}|j}}{\omega_{ji}}\right)\left(\mathbf{r}_{ji}\cos\beta_{ji}+\mathbf{s}_{ji}\sin\beta_{ji}\right) \tag{25}$$

The dot products of Eq. (25) by $\mathbf{u}_{ji}$, $(\mathbf{s}_{ji}\times\mathbf{u}_{ji})\times\mathbf{u}_{ji}$, and $(\mathbf{r}_{ji}\times\mathbf{u}_{ji})\times\mathbf{u}_{ji}$ provide the following explicit expressions of the unknowns

$$ p_{ji}=\left(\frac{{}^iv_{C_{ji}|j}}{\omega_{ji}}\right)\left(\mathbf{r}_{ji}\cos\beta_{ji}+\mathbf{s}_{ji}\sin\beta_{ji}\right)\cdot\mathbf{u}_{ji}=\left(\frac{{}^iv_{C_{ji}|j}}{\omega_{ji}}\right)\cos\beta_{ji}\cdot\cos\gamma_{ji} \tag{26a}$$

$$ x_{ji}=\left(\frac{{}^iv_{C_{ji}|j}}{\omega_{ji}}\right)\frac{\left(\mathbf{r}_{ji}\cos\beta_{ji}+\mathbf{s}_{ji}\sin\beta_{ji}\right)\cdot\left[\left(\mathbf{s}_{ji}\times\mathbf{u}_{ji}\right)\times\mathbf{u}_{ji}\right]}{\left(\mathbf{r}_{ji}\times\mathbf{u}_{ji}\right)\cdot\left[\left(\mathbf{s}_{ji}\times\mathbf{u}_{ji}\right)\times\mathbf{u}_{ji}\right]}=-\left(\frac{{}^iv_{C_{ji}|j}}{\omega_{ji}}\right)\frac{\sin\beta_{ji}}{\sin\gamma_{ji}} \tag{26b}$$

$$ y_{ji}=\left(\frac{{}^iv_{C_{ji}|j}}{\omega_{ji}}\right)\frac{\left(\mathbf{r}_{ji}\cos\beta_{ji}+\mathbf{s}_{ji}\sin\beta_{ji}\right)\cdot\left[\left(\mathbf{r}_{ji}\times\mathbf{u}_{ji}\right)\times\mathbf{u}_{ji}\right]}{\left(\mathbf{s}_{ji}\times\mathbf{u}_{ji}\right)\cdot\left[\left(\mathbf{r}_{ji}\times\mathbf{u}_{ji}\right)\times\mathbf{u}_{ji}\right]}=\left(\frac{{}^iv_{C_{ji}|j}}{\omega_{ji}}\right)\sin\gamma_{ji}\cos\beta_{ji} \tag{26c}$$

where Eq. (23b) has been used to deduce the last formulas. Moreover, the introduction of the last expression of Eq. (26b) into Eq. (24d) yields:

$$ z_{ji}=\left(\frac{{}^iv_{C_{ji}|j}}{\omega_{ji}}\right)\frac{\sin\beta_{ji}}{\cos\gamma_{ji}} \tag{27}$$

Eq. (26a) is the sought-after relationship between p_{ji} and ω_{ji}; whereas, Eqs. (26b), 26c), and ((27) locate ISA_{ji} through the coordinates of its intersections (P and P*) with the tangent plane (C_{ji}, $\mathbf{r}_{ji}$, $\mathbf{s}_{ji}$) and with the second normal plane (C_{ji}, $\mathbf{s}_{ji}$, $\mathbf{t}_{ji}$). Equations (26) and (27) show that, if both $\sin\beta_{ji}=0$ and $\sin\gamma_{ji}=0$, the contact line (C_{ji}, $\mathbf{r}_{ji}$) will be ISA_{ji} and that, if $\sin\beta_{ji}\neq0$ and $\sin\gamma_{ji}=0$, ISA_{ji} will lie on the first normal plane (C_{ji}, $\mathbf{r}_{ji}$, $\mathbf{t}_{ji}$) and be parallel to the contact line (C_{ji}, $\mathbf{r}_{ji}$).

- *Sliding (S_P) contact with a contact point (5 DOF) (Fig. 7)*: in this case, the angular velocity can assume any value and the velocity of the contact point (sliding velocity) cannot have a component along the common normal to the two surfaces that touch each other; therefore, the ISA line can have any direction (i.e., any $\mathbf{u}_{ji}$ is possible) and location in the space (i.e., any A_{ji} is possible); moreover, A_{ji},

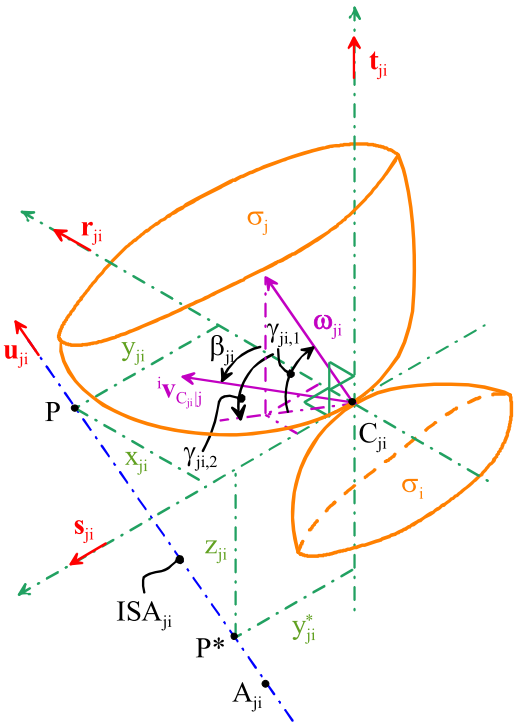

Fig. 7. Sliding contact between links j and i with a contact point (point C_{ji}).

$\mathbf{u}_{ji}$, and p_{ji} are related through a scalar relationship, and ω_{ji} is unknown.

For the S_P pair the relationships among the six parameters that identify the ji relative motion can be deduced as follows. With reference to Fig. 7, σ_j and σ_i are the two surfaces fixed to links j and i, respectively, that touch one another at point C_{ji}; (C_{ji}, $\mathbf{r}_{ji}$, $\mathbf{s}_{ji}$) with $\mathbf{r}_{ji}$ and $\mathbf{s}_{ji}$ that are mutually orthogonal unit vectors is the plane tangent both to σ_j and σ_i at C_{ji} and $\mathbf{t}_{ji}=\mathbf{r}_{ji}\times\mathbf{s}_{ji}$. Accordingly, (C_{ji}, $\mathbf{r}_{ji}$, $\mathbf{t}_{ji}$), and (C_{ji}, $\mathbf{s}_{ji}$, $\mathbf{t}_{ji}$) are the first normal plane, and the second normal plane at the contact point, respectively, of the S_P-pair.

The kinematic conditions, imposed by the S_P-pair, is that the sliding velocity ${}^i\mathbf{v}_{C_{ji}|j}$ must lie on the tangent plane (C_{ji}, $\mathbf{r}_{ji}$, $\mathbf{s}_{ji}$) and that there is no limitation to the direction of $\mathbf{u}_{ji}$. Such conditions yield the following analytic relationships:

$$ {}^i\mathbf{v}_{C_{ji}|j}\cdot\mathbf{t}_{ji}=0 \Rightarrow {}^i\mathbf{v}_{C_{ji}|j}={}^iv_{C_{ji}|j}\left(\mathbf{r}_{ji}\cos\beta_{ji}+\mathbf{s}_{ji}\sin\beta_{ji}\right) \tag{28a}$$

$$ \boldsymbol{\omega}_{ji}=\omega_{ji}\left[\left(\mathbf{r}_{ji}\cos\gamma_{ji,2}+\mathbf{s}_{ji}\sin\gamma_{ji,2}\right)\cos\gamma_{ji,1}+\mathbf{t}_{ji}\sin\gamma_{ji,1}\right]=\omega_{ji}\mathbf{u}_{ji}\Rightarrow\mathbf{u}_{ji}=\left(\mathbf{r}_{ji}\cos\gamma_{ji,2}+\mathbf{s}_{ji}\sin\gamma_{ji,2}\right)\cos\gamma_{ji,1}+\mathbf{t}_{ji}\sin\gamma_{ji,1} \tag{28b}$$

where, ${}^iv_{C_{ji}|j}$ and β_{ji} are the signed magnitude and the angle, respectively, that identify the sliding velocity ${}^i\mathbf{v}_{C_{ji}|j}$ in the tangent plane (C_{ji}, $\mathbf{r}_{ji}$, $\mathbf{s}_{ji}$); whereas, $\gamma_{ji,1}$ and $\gamma_{ji,2}$ are the two angles that uniquely determine the unit vector $\mathbf{u}_{ji}$ (i.e., the direction of ISA_{ji}). Let point P be the intersection between ISA_{ji} and the tangent plane (C_{ji}, $\mathbf{r}_{ji}$, $\mathbf{s}_{ji}$), the following relationships hold (Fig. 7):

$$ {}^i\mathbf{v}_{P|j}={}^i\mathbf{v}_{C_{ji}|j}+\omega_{ji}\left(C_{ji}-P\right)\times\mathbf{u}_{ji} \tag{29a}$$

$$ {}^i\mathbf{v}_{P|j}=p_{ji}\omega_{ji}\mathbf{u}_{ji} \tag{29b}$$

$$ \left(P-C_{ji}\right)=x_{ji}\mathbf{r}_{ji}+y_{ji}\mathbf{s}_{ji} \tag{29c}$$

which are formally similar to Eqs. (24a), (24b), and (24c), but, now, $\mathbf{u}_{ji}$ has the expression given by Eq. (28b). Analogously, the introduction of Eqs. (28a), (29b) and (29c) into Eq. (29a) generates a system of three equations in three unknowns (i.e., p_{ji}, x_{ji} and y_{ji}), which is formally similar to Eq. (25), that is,

$$ p_{ji}\mathbf{u}_{ji}+x_{ji}\mathbf{r}_{ji}\times\mathbf{u}_{ji}+y_{ji}\mathbf{s}_{ji}\times\mathbf{u}_{ji}=\left(\frac{{}^iv_{C_{ji}|j}}{\omega_{ji}}\right)\left(\mathbf{r}_{ji}\cos\beta_{ji}+\mathbf{s}_{ji}\sin\beta_{ji}\right) \tag{30}$$

whose dot products by $\mathbf{u}_{ji}$, $(\mathbf{s}_{ji}\times\mathbf{u}_{ji})\times\mathbf{u}_{ji}$, and $(\mathbf{r}_{ji}\times\mathbf{u}_{ji})\times\mathbf{u}_{ji}$ provide the following explicit expressions of the unknowns computed with the new expression (Eq. (28b)) of $\mathbf{u}_{ji}$

$$p_{ji} = \left(\frac{{}^{i}v_{C_{ji}|j}}{\omega_{ji}}\right)\left(\mathbf{r}_{ji}\cos\beta_{ji} + \mathbf{s}_{ji}\sin\beta_{ji}\right)\cdot\mathbf{u}_{ji} = \left(\frac{{}^{i}v_{C_{ji}|j}}{\omega_{ji}}\right)\left(\cos\beta_{ji}\cos\gamma_{ji,2} + \sin\beta_{ji}\sin\gamma_{ji,2}\right)\cos\gamma_{ji,1} \tag{31a}$$

$$x_{ji} = \left(\frac{{}^{i}v_{C_{ji}|j}}{\omega_{ji}}\right)\frac{\left(\mathbf{r}_{ji}\cos\beta_{ji} + \mathbf{s}_{ji}\sin\beta_{ji}\right)\cdot\left[\left(\mathbf{s}_{ji}\times\mathbf{u}_{ji}\right)\times\mathbf{u}_{ji}\right]}{\left(\mathbf{r}_{ji}\times\mathbf{u}_{ji}\right)\cdot\left[\left(\mathbf{s}_{ji}\times\mathbf{u}_{ji}\right)\times\mathbf{u}_{ji}\right]} = \left(\frac{{}^{i}v_{C_{ji}|j}}{\omega_{ji}}\right)\frac{\cos\beta_{ji}\sin\gamma_{ji,2}\cos\gamma_{ji,2}\cos^2\gamma_{ji,1} - \sin\beta_{ji}\left(\sin^2\gamma_{ji,1} + \cos^2\gamma_{ji,2}\cos^2\gamma_{ji,1}\right)}{\sin\gamma_{ji,1}} \tag{31b}$$

$$y_{ji} = \left(\frac{{}^{i}v_{C_{ji}|j}}{\omega_{ji}}\right)\frac{\left(\mathbf{r}_{ji}\cos\beta_{ji} + \mathbf{s}_{ji}\sin\beta_{ji}\right)\cdot\left[\left(\mathbf{r}_{ji}\times\mathbf{u}_{ji}\right)\times\mathbf{u}_{ji}\right]}{\left(\mathbf{s}_{ji}\times\mathbf{u}_{ji}\right)\cdot\left[\left(\mathbf{r}_{ji}\times\mathbf{u}_{ji}\right)\times\mathbf{u}_{ji}\right]} = \left(\frac{{}^{i}v_{C_{ji}|j}}{\omega_{ji}}\right)\frac{\cos\beta_{ji}\left(\sin^2\gamma_{ji,2}\cos^2\gamma_{ji,1} + \sin^2\gamma_{ji,1}\right) - \sin\beta_{ji}\cos\gamma_{ji,2}\sin\gamma_{ji,2}\cos^2\gamma_{ji,1}}{\sin\gamma_{ji,1}} \tag{31c}$$

Eqs. (31a), (31b), and (31c) are the sought-after relationships. Since both x_{ji} and y_{ji} go to infinity (see Eqs. (31b) and (31c)) when $\mathbf{u}_{ji}$ (i.e., ISA_{ji}) is parallel to the tangent plane (i.e., when $\sin\gamma_{ji,1} = 0$), the computation of the coordinates of the intersection, P*, between ISA_{ji} and the second normal plane (C_{ji}, $\mathbf{s}_{ji}$, $\mathbf{t}_{ji}$) is necessary to solve this indeterminacy. Such coordinates are computable as follows (Fig. 7):

$$\left.\begin{aligned}\left(P^* - C_{ji}\right) &= y^*_{ji}\mathbf{s}_{ji} + z_{ji}\mathbf{t}_{ji}\\ \left(P^* - C_{ji}\right) &= \left(P - C_{ji}\right) + \mu_{ji}\mathbf{u}_{ji} = \left(x_{ji} + \mu_{ji}\cos\gamma_{ji,1}\cos\gamma_{ji,2}\right)\mathbf{r}_{ji} + \left(y_{ji} + \mu_{ji}\sin\gamma_{ji,2}\cos\gamma_{ji,1}\right)\mathbf{s}_{ji} + \mathbf{t}_{ji}\mu_{ji}\sin\gamma_{ji,1}\end{aligned}\right\} \Rightarrow \begin{cases}\mu_{ji} = -\dfrac{x_{ji}}{\cos\gamma_{ji,1}\cos\gamma_{ji,2}}\\ y^*_{ji} = y_{ji} - x_{ji}\tan\gamma_{ji,2}\\ z_{ji} = \mu_{ji}\sin\gamma_{ji,1} = -x_{ji}\dfrac{\tan\gamma_{ji,1}}{\cos\gamma_{ji,2}}\end{cases} \tag{32}$$

where y^*_{ji} and z_{ji} are two scalar parameters that locate P* in the second normal plane (C_{ji}, $\mathbf{s}_{ji}$, $\mathbf{t}_{ji}$). The introduction of formulas (31b) and (31c) into Eqs. (32) yields

$$\begin{cases} y^*_{ji} = \left(\dfrac{{}^{i}v_{C_{ji}|j}}{\omega_{ji}}\right)\dfrac{\sin\gamma_{ji,1}\left(\cos\beta_{ji}\cos\gamma_{ji,2} + \sin\beta_{ji}\sin\gamma_{ji,2}\right)}{\cos\gamma_{ji,2}}\\ z_{ji} = \left(\dfrac{{}^{i}v_{C_{ji}|j}}{\omega_{ji}}\right)\dfrac{\cos\gamma_{ji,1}\left[\sin\beta_{ji}\left(\tan^2\gamma_{ji,1} + \cos^2\gamma_{ji,2}\right) - \cos\beta_{ji}\sin\gamma_{ji,2}\cos\gamma_{ji,2}\right]}{\cos\gamma_{ji,2}}\end{cases} \tag{33}$$

Eventually, it is worth noting that, if pure sliding (i.e., $\omega_{ji}=0$) occurs in a S_L-pair or a S_P-pair, ISA_{ji} will become the line at infinity of the planes perpendicular to the sliding direction given by the unit vector (see Eqs. (23a) and (28a))

$$\tau_{ji} = \mathbf{r}_{ji}\cos\beta_{ji} + \mathbf{s}_{ji}\sin\beta_{ji} \tag{34}$$

2.3. Procedure for the ISA determination in single-DOF spatial mechanisms

The above analysis of the kinematic pairs has highlighted that, in five of them (i.e., R, P, H, C, R_L), which are all the pairs with DOF≤2, ISA_{ji} is completely determined and that in the remaining five (i.e., S, E, R_P, S_L, S_P), ISA_{ji} is partially determined. Therefore, in a mechanism with m links, a simple inspection of the mechanism that just goes through its kinematic pairs allows the determination of a number of ISAs out of the m(m–1)/2 possible ones. By analogy with the IC-determination procedures, the ISAs that can be determined after a simple mechanism inspection will be called "primary" ISAs; whereas, the other ISAs (i.e., the ones whose determination need a specific graphic/analytic procedure) will be called "secondary" ISAs.

The locations of the primary ISAs and the pieces of information on the partially-known secondary ISAs are the input data of the ISA-determination procedure. Such data can be identified directly on a 3D drawing of the mechanism (e.g., through a 3D CAD software) and/or analytically computed by solving the closure-equation system of the mechanism (i.e., its position-analysis problem).

Once the input data have been determined, the determination of the secondary ISAs can be implemented as follows:

i) the indices of all the completely-known ISAs are checked to identify all the four-axes sets that match the hypotheses of the FA theorem[11];
ii) if in step (i) no four-axes set has been determined, jump to step (vi); otherwise continue;
iii) for each four-axes set identified in step (i), the two more ISAs that the FA theorem indicates how to determine are determined through the above-reported formulas that accompany the analytic implementation of the FA theorem;
iv) the secondary ISAs determined in step (iii) are added to the list, L, of the completely-known ISAs;
v) if the updated list L includes all the secondary ISAs, then stop the procedure; otherwise, jump to step (i);
vi) the indices of all the completely-known or partially-known ISAs are checked to identify the four-axes set that, with the minimum number of assigned unknowns, match the hypotheses of the FA theorem;

[11] This step can be implemented by using the same tools (e.g., circle diagrams) employed in single-DOF planar mechanisms to determine the ICs.

vii) for the four-axes set identified in step (vi), the data of the two more ISAs that the FA theorem indicates how to determine are determined as explicit functions of the introduced unknowns and their indices are added to a separate list, L*, of ISAs that are completely known after the introduced unknowns have been determined;
viii) the indices of all the ISAs included in the list $L \cup L*$ are checked to identify all the four-axes sets that match the hypotheses of the FA theorem;
ix) for each four-axes set identified in step (viii) the data of the two more ISAs that the FA theorem indicates how to determine are determined as functions of the introduced unknowns till to generate a system with a number of equations equal to the number of introduced unknowns;
x) the system generated at step (ix) is solved and the computed values of the unknowns are used to compute the data that completely determine the ISAs included in list L*;
xi) all the ISAs included in list L* are added to list L of the completely known ISAs;
xii) clear list L* and jump to step (v).

It is worth stressing that steps (vii) and (ix) need an algebraic manipulator to manage symbolic calculus.

3. Results

In this section, the ISA-determination algorithm presented in Section 2.3 will be applied to two single-DOF spatial mechanisms: the single-loop RCCC mechanism (Fig. 8) and the multi-loop 5-US parallel mechanism (Fig. 9) where U denotes a universal joint (i.e., the combination of two R-pairs with mutually orthogonal and intersecting axes that are connected in series).

3.1. Determination of the secondary ISAs in the RCCC mechanism

In the literature (see, for instance, [20,25,30–34]), RCCC mechanisms have been extensively studied. An RCCC mechanism (Fig. 8 (a)) features four binary links connected in a single-loop through one R-pair and three C-pairs. In Fig. 8(a), link 1 is the frame and link 2 is connected to the frame through the unique R-pair. Accordingly, the total number of possible relative motions is 6 (=4(4–1)/2) and the corresponding ISAs are ISA_{21}, ISA_{32}, ISA_{43}, ISA_{41}, ISA_{31}, and ISA_{42}. With reference to the geometric constraints on ISAs listed in Section 2.2, the simple inspection of the RCCC mechanism reveals that ISA_{21} ($\equiv(A_{21}, \mathbf{u}_{21})$ in Fig. 8(a)), ISA_{32} ($\equiv(A_{32}, \mathbf{u}_{32})$ in Fig. 8(a)), ISA_{43} ($\equiv(A_{43}, \mathbf{u}_{43})$ in Fig. 8(a)), and ISA_{41} ($\equiv(A_{41}, \mathbf{u}_{41})$ in Fig. 8(a)) are primary ISAs and the remaining two, that is, ISA_{31} and ISA_{42}, are the secondary ISAs whose location must be determined.

The four known ISAs respect the above-stated rule 2. Accordingly, the FA theorem can be applied to them. In particular, the set of primary-ISA indices is {21, 32, 43, 41}. Thus, the application of the FA theorem to the two ISA pairs (ISA_{21}, ISA_{32}) and (ISA_{41}, ISA_{43}) brings to determine ISA_{31}; whereas, the application of the FA theorem to the two ISA pairs (ISA_{21}, ISA_{41}) and (ISA_{43}, ISA_{32}) brings to determine ISA_{42}. This analysis of the ISA-indices is immediately implementable through the circle diagram shown in Fig. 8(b) that is built by using the same rules adopted for the circle diagrams when they are employed for determining secondary ICs in planar mechanisms [27,28]. In short, the numbers refer to the links and the segments that join two numbers refer to the already-determined ISAs; consequently, every quadrilateral of already-determined ISAs respect rule 2 and indicates that the two ISAs associated to the two diagonals of the quadrilateral can be determined through the FA theorem.

The geometric determination of ISA_{31} and ISA_{42} is reported in Fig. 8(a) where the line (Q_{31}, $\mathbf{u}_{31}$) (the line (Q_{42}, $\mathbf{u}_{42}$)) is ISA_{31} (ISA_{42}) and has been determined as common normal to the lines (Q_{32}, $\mathbf{n}_2$) and (Q'_{43}, $\mathbf{n}_4$) (to the lines (Q_{43}, $\mathbf{n}_3$) and (Q_{41}, $\mathbf{n}_1$)). The analytic determination of ISA_{31} and ISA_{42} is also straight since, after the closure-equation system has been numerically or analytically solved, it simply consists in using the explicit formulas (19) and (21) two times, one for ISA_{31} and the other for ISA_{42}. This analytic determination is reported in the remaining part of this subsection.

With reference to Fig. 8(a), the unit vectors $\mathbf{u}_{21}$, $\mathbf{u}_{41}$ and $\mathbf{n}_1$ ($\equiv \mathbf{u}_{41} \times \mathbf{u}_{21} / \| \mathbf{u}_{41} \times \mathbf{u}_{21} \| = \mathbf{u}_{41} \times \mathbf{u}_{21} / \sin\alpha_{41,21}$) are fixed to the frame and the following relationships hold:

$$\mathbf{n}_2 = \mathbf{n}_1\cos\theta_{21} + (\mathbf{n}_1 \times \mathbf{u}_{21})\sin\theta_{21} = \frac{\mathbf{u}_{32} \times \mathbf{u}_{21}}{\sin\alpha_{32,21}};\ \mathbf{u}_{32} = \mathbf{u}_{21}\cos\alpha_{32,21} + (\mathbf{u}_{21} \times \mathbf{n}_2)\sin\alpha_{32,21}; \tag{35a}$$

$$\mathbf{n}_3 = \mathbf{n}_2\cos\theta_{32} + (\mathbf{n}_2 \times \mathbf{u}_{32})\sin\theta_{32} = \frac{\mathbf{u}_{32} \times \mathbf{u}_{43}}{\sin\alpha_{32,43}};\ \mathbf{u}_{43} = \mathbf{u}_{32}\cos\alpha_{32,43} - (\mathbf{u}_{32} \times \mathbf{n}_3)\sin\alpha_{32,43}; \tag{35b}$$

$$\mathbf{u}_{43} \cdot \mathbf{u}_{41} = \cos\alpha_{43,41} \tag{35c}$$

$$\left.\begin{array}{l} \mathbf{u}_{43} = \mathbf{u}_{32}\cos\alpha_{32,43} - (\mathbf{u}_{32} \times \mathbf{n}_3)\sin\alpha_{32,43} \\ \mathbf{n}_4 = \mathbf{n}_1\cos\theta_{41} + (\mathbf{n}_1 \times \mathbf{u}_{41})\sin\theta_{41} \\ \mathbf{u}_{43} = \mathbf{u}_{41}\cos\alpha_{43,41} + (\mathbf{u}_{41} \times \mathbf{n}_4)\sin\alpha_{43,41} \end{array}\right\} \Rightarrow \mathbf{u}_{32}\cos\alpha_{32,43} - (\mathbf{u}_{32} \times \mathbf{n}_3)\sin\alpha_{32,43} = \mathbf{u}_{41}\cos\alpha_{43,41} + (\mathbf{u}_{41} \times \mathbf{n}_4)\sin\alpha_{43,41} \tag{35d}$$

$$\left.\begin{array}{l} \mathbf{n}_4 = \mathbf{n}_3\cos\theta_{43} + (\mathbf{n}_3 \times \mathbf{u}_{43})\sin\theta_{43} \\ \mathbf{n}_4 = \mathbf{n}_1\cos\theta_{41} + (\mathbf{n}_1 \times \mathbf{u}_{41})\sin\theta_{41} \end{array}\right\} \Rightarrow \mathbf{n}_3\cos\theta_{43} + (\mathbf{n}_3 \times \mathbf{u}_{43})\sin\theta_{43} = \mathbf{n}_1\cos\theta_{41} + (\mathbf{n}_1 \times \mathbf{u}_{41})\sin\theta_{41} \tag{35e}$$

$$a_1\mathbf{n}_1 + d_1\mathbf{u}_{21} - a_2\mathbf{n}_2 - d_{32}\mathbf{u}_{32} - a_3\mathbf{n}_3 - d_{43}\mathbf{u}_{43} + a_4\mathbf{n}_4 - d_{41}\mathbf{u}_{41} = \mathbf{0} \tag{35f}$$

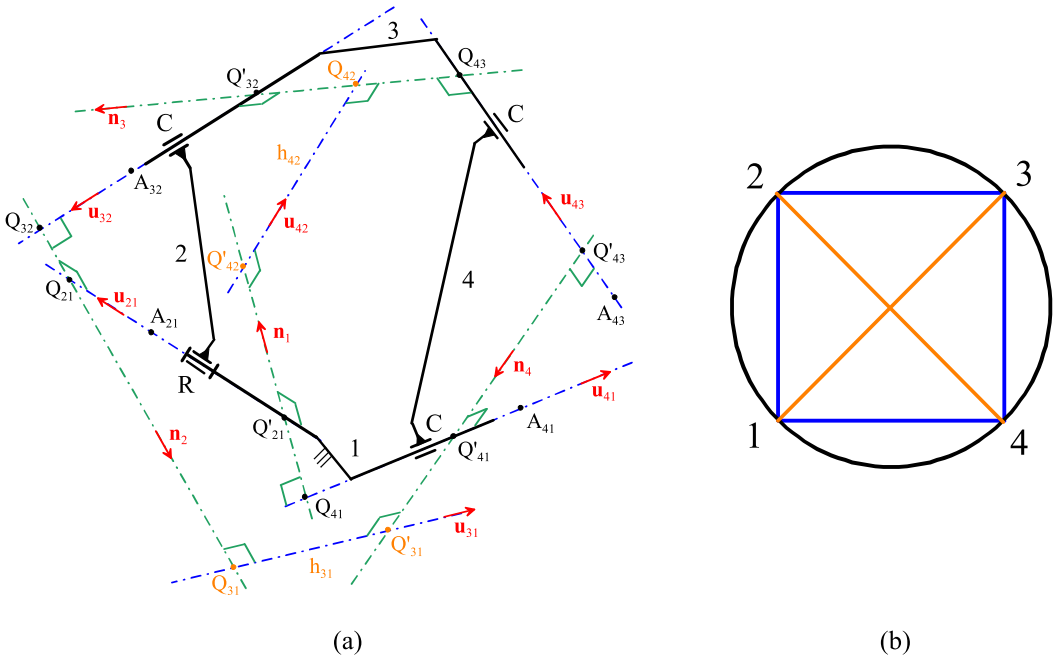

Fig. 8. The RCCC mechanism: (a) kinematic scheme of the mechanism with the geometric determination of the secondary ISAs, (b) circle diagram of the RCCC mechanism (the blue segments refer to the primary ISAs (i.e., $ISA_{21}\equiv(A_{21}, u_{21})$, $ISA_{32}\equiv(A_{32}, u_{32})$, $ISA_{43}\equiv(A_{43}, u_{43})$, and $ISA_{41}\equiv(A_{41}, u_{41})$); the brown segments refer to the secondary ISAs (i.e., $ISA_{31}\equiv(Q_{31}, u_{31})$, and $ISA_{42}\equiv(Q_{42}, u_{42})$)).

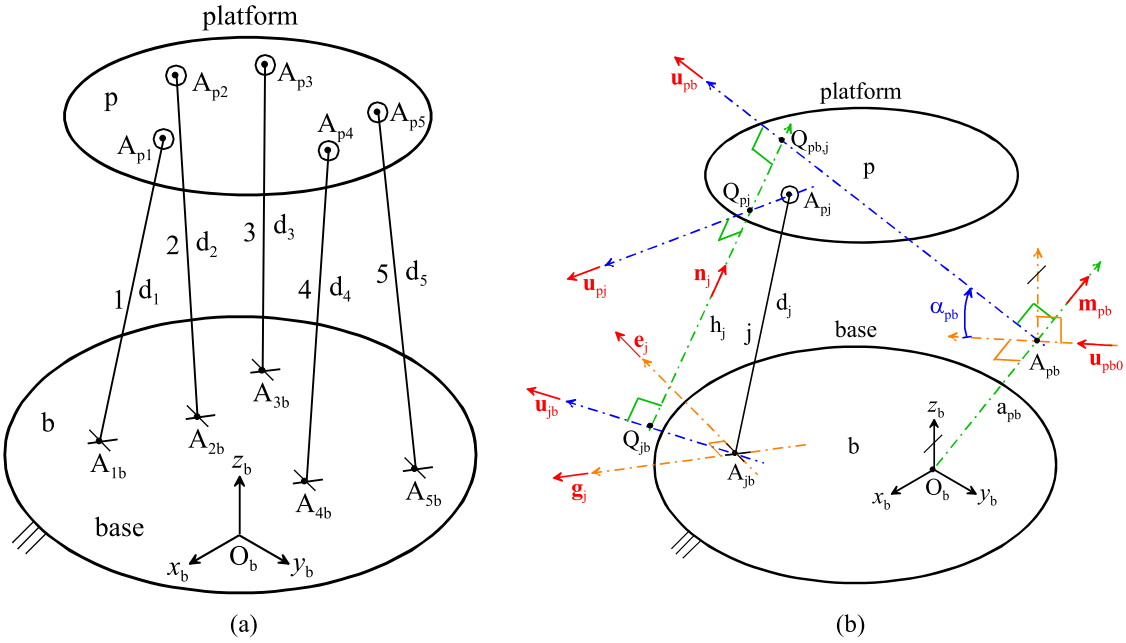

Fig. 9. The 5-US parallel mechanism (U stands for Universal joint; A_{jb} and A_{pj}, for j =1,2,…,5, are the centers of the U-joint and of the S-pair, respectively, in the j-th limb): (a) kinematic scheme, (b) limb j, j =1,2,…,5, and adopted notations.

where the angles $\alpha_{41,21}$, $\alpha_{32,21}$, $\alpha_{32,43}$ and $\alpha_{43,41}$ are geometric constants of the links 1, 2, 3 and 4, respectively, and the angle θ_{ji}, for ji$\in$ {21, 32, 43, 41}, is a joint variable defined as the rotation angle around ISA_{ji} that is positive if counterclockwise with respect to $\mathbf{u}_{ji}$ and equal to zero when $\mathbf{n}_j = \mathbf{n}_i$. Moreover, in Eq. (35f), the linear parameters a_1, d_1, a_2, a_3 and a_4 are geometric constants of the links defined as follows (see Fig. 8(a)):

$$a_1 = \left(\dot{Q_{21}} - Q_{41}\right) \cdot \mathbf{n}_1;\ d_1 = \left(Q_{21} - \dot{Q_{21}}\right) \cdot \mathbf{u}_{21};\ a_2 = \left(Q_{21} - Q_{32}\right) \cdot \mathbf{n}_2; \tag{36a}$$

$$a_3 = \left(\dot{Q_{32}} - Q_{43}\right) \cdot \mathbf{n}_3;\ a_4 = \left(\dot{Q_{41}} - \dot{Q_{43}}\right) \cdot \mathbf{n}_4; \tag{36b}$$

whereas, the linear parameters d_{32}, d_{43} and d_{41} are joint variables defined as follows (see Fig. 8(a)):

$$d_{32} = \left(Q_{32} - \dot{Q_{32}}\right) \cdot \mathbf{u}_{32};\ d_{43} = \left(Q_{43} - \dot{Q_{43}}\right) \cdot \mathbf{u}_{43};\ d_{41} = \left(\dot{Q_{41}} - Q_{41}\right) \cdot \mathbf{u}_{41}. \tag{37}$$

The position analysis of an RCCC mechanism is solvable in closed form [30] and provides at most two solutions for each assigned value of the generalized coordinate. Eqs. (35c)–(35f) can be used to solve it as follows. Let θ_{21} be the chosen generalized coordinate, the introduction of formulas (35a) and (35b) into Eq. (35c), after some algebraic manipulations, yields

$$b_0 + b_1 \sin\theta_{32} + b_2 \cos\theta_{32} = 0 \tag{38}$$

where

$$b_0 = \left(\cos\alpha_{41,21}\cos\alpha_{32,21} + \sin\alpha_{41,21}\sin\alpha_{32,21}\cos\theta_{21}\right)\cos\alpha_{32,43} - \cos\alpha_{43,41}; \tag{39a}$$

$$b_1 = \sin\alpha_{41,21}\sin\alpha_{32,43}\sin\theta_{21};\ b_2 = \left(\cos\alpha_{41,21}\sin\alpha_{32,21} - \sin\alpha_{41,21}\cos\alpha_{32,21}\cos\theta_{21}\right)\sin\alpha_{32,43}. \tag{39b}$$

Then, the introduction of the trigonometric identities $\sin\theta_{32}=2t/(1+t^2)$ and $\cos\theta_{32}=(1-t^2)/(1+t^2)$, with $t=\tan(\theta_{32}/2)$, into Eq. (38) makes it a quadratic equation in t whose solution provides the following two explicit expressions of θ_{32} as a function of θ_{21} and of the geometric constants

$$\theta_{32,k} = 2\arctan\left(\frac{-b_1 + (-1)^k\sqrt{{b_1}^2 + {b_2}^2 - {b_0}^2}}{b_0 - b_2}\right) k = 1, 2 \tag{40}$$

The introduction into Eq. (35d) of the computed values (θ_{21}, $\theta_{32,k}$) allows the computation of the corresponding $\theta_{41,k}$ through the following explicit formula

$$\theta_{41,k} = \operatorname{atan2}\left(\frac{\mathbf{u}_{43,k} \cdot \mathbf{n}_1}{\sin\alpha_{43,41}}, \frac{\mathbf{u}_{41} \cdot \left(\mathbf{n}_1 \times \mathbf{u}_{43,k}\right)}{\sin\alpha_{43,41}}\right) k = 1, 2 \tag{41}$$

where

$$\mathbf{u}_{43,k} \cdot \mathbf{n}_1 = \sin\alpha_{32,21}\cos\alpha_{32,43}\sin\theta_{21} - \left(\sin\theta_{21}\cos\theta_{32,k}\cos\alpha_{32,21} + \cos\theta_{21}\sin\theta_{32,k}\right)\sin\alpha_{32,43} \tag{42a}$$

$$\begin{aligned}\mathbf{u}_{41} \cdot \left(\mathbf{n}_1 \times \mathbf{u}_{43,k}\right) = {} & \cos\alpha_{41,21}\left[\sin\alpha_{32,21}\cos\alpha_{32,43}\cos\theta_{21} + \left(\sin\theta_{21}\sin\theta_{32,k} - \cos\theta_{21}\cos\theta_{32,k}\cos\alpha_{32,21}\right)\sin\alpha_{32,43}\right] + \\ & -\sin\alpha_{41,21}\left(\cos\alpha_{32,21}\cos\alpha_{32,43} + \sin\alpha_{32,21}\sin\alpha_{32,43}\cos\theta_{32,k}\right)\end{aligned} \tag{42b}$$

Eventually, the introduction into Eq. (35e) of the computed values (θ_{21}, $\theta_{32,k}$, $\theta_{41,k}$) allows the computation of the corresponding $\theta_{43,k}$ through the following explicit formula

$$\theta_{43,k} = \operatorname{atan2}\left(\left[\mathbf{n}_1\cos\theta_{41,k} + (\mathbf{n}_1 \times \mathbf{u}_{41})\sin\theta_{41,k}\right] \cdot \left(\mathbf{n}_{3,k} \times \mathbf{u}_{43,k}\right),\ \left[\mathbf{n}_1\cos\theta_{41,k} + (\mathbf{n}_1 \times \mathbf{u}_{41})\sin\theta_{41,k}\right] \cdot \mathbf{n}_{3,k}\right),\ k = 1, 2 \tag{43}$$

where

$$\begin{aligned}\left[\mathbf{n}_1\cos\theta_{41,k} + (\mathbf{n}_1 \times \mathbf{u}_{41})\sin\theta_{41,k}\right] \cdot \left(\mathbf{n}_{3,k} \times \mathbf{u}_{43,k}\right) = {} & \left(\cos\theta_{21}\cos\theta_{32,k} - \sin\theta_{21}\sin\theta_{32,k}\cos\alpha_{32,21}\right)\left(cos^2\theta_{41,k}\sin\alpha_{43,41} + \cos\alpha_{43,41}\sin\theta_{41,k}\right) + \\ & -\left(\cos\alpha_{41,21}\cos\alpha_{43,41}\cos\theta_{41,k} - \sin\alpha_{41,21}\sin\alpha_{43,41}sin^2\theta_{41,k}\right)\left(\sin\theta_{21}\cos\theta_{32,k} + \cos\theta_{21}\sin\theta_{32,k}\cos\alpha_{32,21}\right) + \\ & -\left(\sin\alpha_{41,21}\cos\alpha_{43,41}\cos\theta_{41,k} + \cos\alpha_{41,21}\sin\alpha_{43,41}sin^2\theta_{41,k}\right)\sin\alpha_{32,21}\sin\theta_{32,k}\end{aligned} \tag{44a}$$

$$\begin{aligned}\left[\mathbf{n}_1\cos\theta_{41,k} + (\mathbf{n}_1 \times \mathbf{u}_{41})\sin\theta_{41,k}\right] \cdot \mathbf{n}_{3,k} = {} & \left(\cos\theta_{21}\cos\theta_{32,k} - \sin\theta_{21}\sin\theta_{32,k}\cos\alpha_{32,21}\right)\cos\theta_{41,k} + \\ & +\left[\cos\alpha_{41,21}\left(\sin\theta_{21}\cos\theta_{32,k} + \cos\theta_{21}\sin\theta_{32,k}\cos\alpha_{32,21}\right) + \sin\alpha_{41,21}\sin\alpha_{32,21}\sin\theta_{32,k}\right]\sin\theta_{41,k}\end{aligned} \tag{44b}$$

Finally, the introduction into Eq. (35f) of the computed values (θ_{21}, $\theta_{32,k}$, $\theta_{41,k}$, $\theta_{43,k}$), k=1, 2, makes it the linear system of three equations in the remaining three unknowns, $d_{32,k}$, $d_{43,k}$ and $d_{41,k}$, that follows

$$d_{32,k}\mathbf{u}_{32} + d_{43,k}\mathbf{u}_{43,k} + d_{41,k}\mathbf{u}_{41} = \mathbf{c}_k\ k = 1,\ 2 \tag{45}$$

with $\mathbf{c}_k = a_1\mathbf{n}_1 + d_1\mathbf{u}_{21} - a_2\mathbf{n}_2 - a_3\mathbf{n}_{3,k} + a_4\mathbf{n}_{4,k}$, whose solutions are

$$d_{32,k} = \frac{\mathbf{c}_k \cdot \left(\mathbf{u}_{43,k} \times \mathbf{u}_{41}\right)}{\mathbf{u}_{32} \cdot \left(\mathbf{u}_{43,k} \times \mathbf{u}_{41}\right)};\ d_{43,k} = \frac{\mathbf{c}_k \cdot \left(\mathbf{u}_{32} \times \mathbf{u}_{41}\right)}{\mathbf{u}_{43,k} \cdot \left(\mathbf{u}_{32} \times \mathbf{u}_{41}\right)};\ d_{41,k} = \frac{\mathbf{c}_k \cdot \left(\mathbf{u}_{32} \times \mathbf{u}_{43,k}\right)}{\mathbf{u}_{41} \cdot \left(\mathbf{u}_{32} \times \mathbf{u}_{43,k}\right)}.\ k = 1, 2 \tag{46}$$

Eqs. (40), (41), (43) and (46), which must be used in sequence, provide the closed-form solutions of the RCCC position analysis.

Table 1
Numerical example of a RCCC mechanism: position analysis solutions for $\theta_{21}=1.25\pi$ rad (l.u. stands for generic length unit).

k	$\theta_{32,k}$ [rad]	$\theta_{41,k}$ [rad]	$\theta_{43,k}$ [rad]	$d_{32,k}$ [l.u.]	$d_{43,k}$ [l.u.]	$d_{41,k}$ [l.u.]
1	0	π	-0.25π	−3.5858	3	−6.0711
2	$-\pi$	π	0.75π	2.4142	3	2.4142

Once all the joint variables have been computed as a function of the generalized coordinate θ_{21}, the directions of $ISA_{31}\equiv(Q_{31}, \mathbf{u}_{31})$ and $ISA_{42}\equiv(Q_{42}, \mathbf{u}_{42})$, for each of the two position-analysis solutions, are (see Eq. (19c) and Figs. 4 and 8(a))

$$\mathbf{u}_{31,k}=\frac{\mathbf{n}_2\times\mathbf{n}_{4,k}}{\|\mathbf{n}_2\times\mathbf{n}_{4,k}\|};\ \mathbf{u}_{42,k}=\frac{\mathbf{n}_{3,k}\times\mathbf{n}_1}{\|\mathbf{n}_{3,k}\times\mathbf{n}_1\|};\ k=1,2 \tag{47}$$

whereas their positions are located as follows (see Eqs. (19b), (20) and (21) and Figs. 4 and 8(a))

$$Q_{31,k}=Q_{21}+\left(y_{Q_{31,k}}-a_2\right)\mathbf{n}_2;\ Q_{42,k}=Q_{41}+y_{Q'_{42,k}}\mathbf{n}_1+h_{42,k}\mathbf{u}_{42,k};\ k=1,2 \tag{48}$$

with (see Fig. 8(a))

$$y_{Q'_{31,k}}\mathbf{n}_{4,k}-y_{Q_{31,k}}\mathbf{n}_2-h_{31,k}\mathbf{u}_{31,k}=\left(Q_{32}-Q'_{43,k}\right)\Rightarrow\begin{cases}h_{31,k}=-\left(Q_{32}-Q'_{43,k}\right)\cdot\mathbf{u}_{31,k}\\ y_{Q'_{31,k}}=\dfrac{\left(Q_{32}-Q'_{43,k}\right)\cdot\left(\mathbf{n}_2\times\mathbf{u}_{31,k}\right)}{\mathbf{n}_{4,k}\cdot\left(\mathbf{n}_2\times\mathbf{u}_{31,k}\right)}\\ y_{Q_{31,k}}=-\dfrac{\left(Q_{32}-Q'_{43,k}\right)\cdot\left(\mathbf{n}_{4,k}\times\mathbf{u}_{31,k}\right)}{\mathbf{n}_2\cdot\left(\mathbf{n}_{4,k}\times\mathbf{u}_{31,k}\right)}\end{cases}k=1,2 \tag{49a}$$

$$y_{Q'_{42,k}}\mathbf{n}_1-y_{Q_{42,k}}\mathbf{n}_{3,k}+h_{42,k}\mathbf{u}_{42,k}=\left(Q_{43,k}-Q_{41}\right)\Rightarrow\begin{cases}h_{42,k}=\left(Q_{43,k}-Q_{41}\right)\cdot\mathbf{u}_{42,k}\\ y_{Q'_{42,k}}=\dfrac{\left(Q_{43,k}-Q_{41}\right)\cdot\left(\mathbf{n}_{3,k}\times\mathbf{u}_{42,k}\right)}{\mathbf{n}_1\cdot\left(\mathbf{n}_{3,k}\times\mathbf{u}_{42,k}\right)}\\ y_{Q_{42,k}}=-\dfrac{\left(Q_{43,k}-Q_{41}\right)\cdot\left(\mathbf{n}_1\times\mathbf{u}_{42,k}\right)}{\mathbf{n}_{3,k}\cdot\left(\mathbf{n}_1\times\mathbf{u}_{42,k}\right)}\end{cases}k=1,2 \tag{49b}$$

where

$$Q_{32}=Q_{21}-a_2\,\mathbf{n}_2;\ Q'_{43,k}=Q_{41}+d_{41,k}\mathbf{u}_{41}-a_4\,\mathbf{n}_{4,k};\ Q_{43,k}=Q'_{43,k}+d_{43,k}\mathbf{u}_{43,k}. \tag{50}$$

Eqs. (47) and (48) provide the explicit expressions of the sought-after ISA locations as a function of the generalized coordinate.

The above-reported formulas have been tested with the following RCCC-mechanism's geometric data (l.u. stands for a generic length unit): $A_{21}=(0,0,0)^T$ l.u., $\mathbf{u}_{21}=(0,1,0)^T$ l.u., $d_1=3$ l.u., $A_{41}=(0,0,-1)^T$ l.u., $\mathbf{u}_{21}=(1,0,0)^T$ l.u., $a_2=2$ l.u., $\alpha_{32,21}=0.5\pi$ rad, $a_3=3$ l.u., $\alpha_{32,43}=0.5\pi$ rad, $a_4=2$ l.u., $\alpha_{43,41}=0.5\pi$ rad. With these geometric data the two position analysis solutions for $\theta_{21}=1.25\pi$ rad are reported in Table 1; whereas, Fig. 10 shows the RCCC mechanism in the two corresponding configurations together with the locations of ISA_{31} and ISA_{42}.

3.2. Determination of the secondary ISAs in the 5-US parallel mechanism

The 5-US parallel mechanism (see Fog. 9(a)) features a mobile rigid-body (platform) connected to the frame (base) through five kinematic chains (limbs) of type US (i.e., constituted by one binary link whose endings are joined to the platform with one S-pair and to the base with one U-joint). In each limb, the line passing through the centers of the U-joint and of the S-pair is the limb axis; the U-joint just makes the limb rotation around its axis controllable and it has no effect on the relative motion between platform (link p in Fig. 9) and base (link b in Fig. 9), which is the same as the one of the 5-SS parallel mechanism. In the literature, the interest for the 5-US mechanism is mainly related to multi-link suspensions [35–41] of ground vehicles and to human-knee modeling [42].

With reference to Fig. 9, link j for j=1,…,5 is the binary link of the j-th limb; link p (link b) is the platform (the base). Moreover, A_{jb} (A_{pj}) for j=1,…,5 is the center of the U-joint (of the S-pair) of the j-th limb and d_j for j=1,…,5 is the length (limb length) of the segment $A_{jb}A_{pj}$. Eventually, $\mathbf{e}_j$ and $\mathbf{g}_j$ for j=1,…,5 are the unit vectors of the two R-pair axes of the U-joint belonging to the j-th limb.

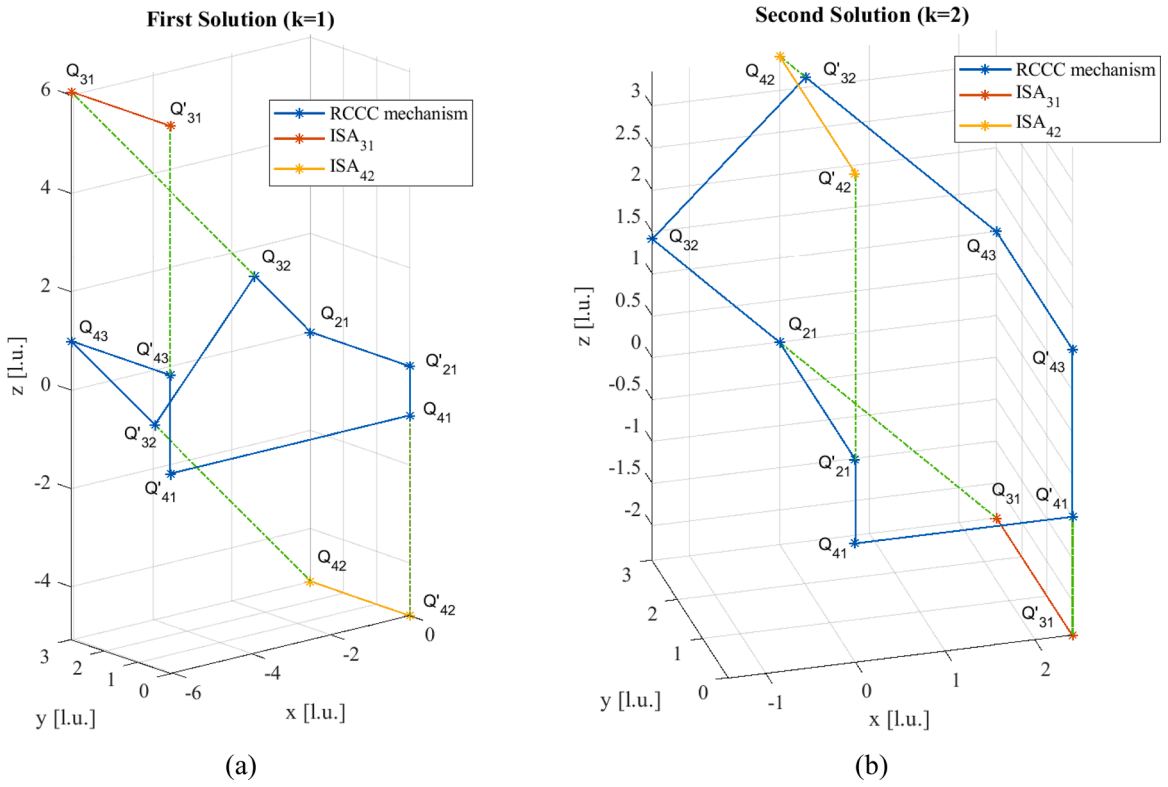

Fig. 10. Numerical example of a RCCC mechanism: (a) RCCC mechanism at the 1st position-analysis solution together with ISA_{31} and ISA_{42}, (b) RCCC mechanism at the 2nd position-analysis solution together with ISA_{31} and ISA_{42}.

The mechanism inspection and the geometric constraints on the ISAs reported in Section 2.2 bring one to conclude that A_{pj} (see Fig. 9(b)) must belong to ISA_{pj} (i.e., $ISA_{pj} \equiv (A_{pj}, \mathbf{u}_{pj})$), and that ISA_{jb} must lie on the plane (A_{jb}, $\mathbf{e}_j$, $\mathbf{g}_j$)[12] and must pass through point A_{jb} (i.e., $ISA_{jb} \equiv (A_{jb}, \mathbf{u}_{jb})$ with $\mathbf{u}_{jb} \cdot (\mathbf{e}_j \times \mathbf{g}_j) = 0$). Therefore, in the 5-US mechanism, there is no primary ISA and ten secondary ISAs (i.e., $ISA_{pj} \equiv (A_{pj}, \mathbf{u}_{pj})$ and $ISA_{jb} \equiv (A_{jb}, \mathbf{u}_{jb})$ for j=1,…,5) are partially known. As a consequence, the determination of the secondary ISAs must be done by exploiting steps (vi)–(xii) of the algorithm presented in Section 2.3. In the 5-US mechanism, the total number of ISAs is 21 (=7(7–1)/2), but only the $ISA_{pb} \equiv (A_{pb}, \mathbf{u}_{pb})$ is of interest in its applications. Accordingly, only the ISA_{pb} determination will be discussed in details in the following part of this subsection.

The position analysis of the 5-US mechanism can be addressed through the algorithms conceived to solve the direct position analysis of particular fully-parallel-manipulators (FPMs) [43]. Indeed, assigning the value of one joint variable (i.e., the one chosen as generalized coordinate for this single-DOF spatial mechanism) corresponds to the introduction of a sixth (fictitious) limb (see Fig. 11) for locking the 5-US mechanism at a given configuration and the so-generated spatial structure coincides with the one obtained from the 6–5 FPM [44–46], which has six DOF, by locking the six limb lengths. Such a problem can be solved only in analytical form (i.e., through an algorithm with a definite number of algebraic operations that computes all the possible solutions) and admits at most 40 solutions (see [45,46] for details). Despite the complexity of the algebraic solution, the closure-equation system can be put in the following simple form (Fig. 11)

$$\left(A_{p1} + {}^{b}\mathbf{R}_{p}\,{}^{p}A_{pj} - A_{jb}\right) \cdot \left(A_{p1} + {}^{b}\mathbf{R}_{p}\,{}^{p}A_{pj} - A_{jb}\right) = d_j^2,\ j = 0, 1, \cdots, 5 \tag{51}$$

where $A_{p0} \equiv A_{p1}$, ${}^{b}\mathbf{R}_{p}$ is the rotation matrix that transforms vector components measured in $A_{p1}x_p y_p z_p$ into components of the same vector measured in $O_b x_b y_b z_b$ (see Fig. 11), A_{pj} (${}^{p}A_{pj}$) for j=0, 1,…,5 is the position vector of point A_{pj} measured in $O_b x_b y_b z_b$ (measured in $A_{p1}x_p y_p z_p$) and A_{jb} for j=0, 1,…,5 is the position vector of point A_{jb} measured in $O_b x_b y_b z_b$. In system (51), d_0 plays the role of generalized coordinate; A_{p1} and the orientation parameters that uniquely identify ${}^{b}\mathbf{R}_{p}$ are the unknowns to compute[13]; whereas ${}^{p}A_{pj}$ and A_{jb} for j=0, 1,…,5 are known constant vectors that define the geometry of the platform and the base, respectively.

If one is interested only to mechanism configurations near to a reference configuration as in the study of a car suspension, system

[12] It is worth noting that, if the spatial disposition of the U-joint is not of interest as it happens in the case of a suspension, the rotation of limb j around its axis can be locked by imposing that $\mathbf{e}_j$ and $\mathbf{g}_j$ be both perpendicular to the j-th limb axis. In general, such a condition is numerically more efficient since it eliminates the U-joint singularity, which occurs when the j-th limb axis (i.e., point A_{pj}) lies on the plane (A_{jb}, $\mathbf{e}_j$, $\mathbf{g}_j$).

[13] It is worth reminding that $A_{pj} = A_{p1} + {}^{b}\mathbf{R}_{p}\,{}^{p}A_{pj}$

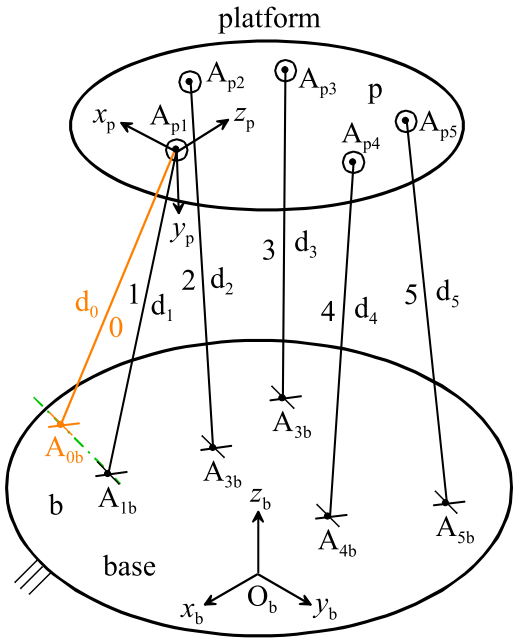

Fig. 11. Locking one joint variable of the 5-US mechanism modelled through the introduction of one fictitious limb (limb 0) for freezing the 5-US mechanism at a configuration (the reference systems $O_b x_b y_b z_b$ and $A_{p1} x_p y_p z_p$ are fixed to base and platform, respectively).

(51) can be solved numerically starting from the reference configuration and using numerical algorithms for the solution of non-linear system of equations (e.g., Newton-Raphson method [47]). Once the position analysis of the 5-US mechanism has been solved the ISA_{pb} determination can start.

Fig. 9(b) shows the j-th limb together with $ISA_{jb} \equiv (A_{jb}, \mathbf{u}_{jb})$ and $ISA_{pj} \equiv (A_{pj}, \mathbf{u}_{pj})$, which are the two partially-known secondary ISAs referable to the j-th limb, and the geometric relationship, due to the EAK theorem, between these two partially-known ISAs and $ISA_{pb} \equiv (A_{pb}, \mathbf{u}_{pb})$, which is the unknown secondary ISA to determine. With reference to Fig. 9(b), after the position-analysis solution, the coordinates of points A_{pj} and the components of unit vectors $\mathbf{e}_j$ and $\mathbf{g}_j$, for j=1,…,5, are all known in the reference system $O_b x_b y_b z_b$. By using these data the following relationships can be written (see Eq. (A.4) of Appendix A and Eq. (1b))

$$\mathbf{m}_{pb} = \left(\mathbf{i}_b \cos\gamma_{pb} + \mathbf{j}_b \sin\gamma_{pb}\right)\cos\beta_{pb} + \mathbf{k}_b \sin\beta_{pb}; A_{pb} = a_{pb}\mathbf{m}_{pb}; \tag{52a}$$

$$\mathbf{u}_{pb0} = \frac{\mathbf{k}_b \times \mathbf{m}_{pb}}{\| \mathbf{k}_b \times \mathbf{m}_{pb} \|}; \; \mathbf{u}_{pb} = \mathbf{u}_{pb0}\cos\alpha_{pb} + \left(\mathbf{m}_{pb} \times \mathbf{u}_{pb0}\right)\sin\alpha_{pb}; \tag{52b}$$

$$\mathbf{u}_{jb} = \mathbf{e}_j \cos\beta_{jb} + \mathbf{g}_j \sin\beta_{jb}; \; \mathbf{n}_j = \frac{\mathbf{u}_{jb} \times \mathbf{u}_{pb}}{\| \mathbf{u}_{jb} \times \mathbf{u}_{pb} \|}; \; j = 1, \cdots, 5 \tag{52c}$$

$$\begin{cases} Q_{pb,j} = A_{pb} + \dfrac{\left(A_{jb} - A_{pb}\right) \cdot \left[\mathbf{u}_{pb} - \left(\mathbf{u}_{jb} \cdot \mathbf{u}_{pb}\right)\mathbf{u}_{jb}\right]}{1 - \left(\mathbf{u}_{jb} \cdot \mathbf{u}_{pb}\right)^2}\mathbf{u}_{pb} = A_{pb} + \dfrac{\left(A_{jb} - A_{pb}\right) \cdot \left(\mathbf{u}_{pb} - \mathbf{u}_{jb}\cos\alpha_{pb,jb}\right)}{\sin^2\alpha_{pb,jb}}\mathbf{u}_{pb} \\ Q_{jb} = A_{jb} + \dfrac{\left(A_{pb} - A_{jb}\right) \cdot \left[\mathbf{u}_{jb} - \left(\mathbf{u}_{jb} \cdot \mathbf{u}_{pb}\right)\mathbf{u}_{pb}\right]}{1 - \left(\mathbf{u}_{jb} \cdot \mathbf{u}_{pb}\right)^2}\mathbf{u}_{jb} = A_{jb} + \dfrac{\left(A_{pb} - A_{jb}\right) \cdot \left(\mathbf{u}_{jb} - \mathbf{u}_{pb}\cos\alpha_{pb,jb}\right)}{\sin^2\alpha_{pb,jb}}\mathbf{u}_{jb} \end{cases} \quad j = 1, \cdots, 5 \tag{52d}$$

$$y_j = \left(Q_{pb,j} - Q_{jb}\right) \cdot \mathbf{n}_j; \; h_j = \left(A_{pj} - Q_{jb}\right) \cdot \mathbf{n}_j; \; j = 1, \cdots, 5 \tag{52e}$$

$$Q_{pj} = Q_{jb} + h_j \mathbf{n}_j = Q_{jb} + \left[\frac{\left(A_{pj} - Q_{jb}\right) \cdot \left(\mathbf{u}_{jb} \times \mathbf{u}_{pb}\right)}{\left(\mathbf{u}_{jb} \times \mathbf{u}_{pb}\right) \cdot \left(\mathbf{u}_{jb} \times \mathbf{u}_{pb}\right)}\right]\left(\mathbf{u}_{jb} \times \mathbf{u}_{pb}\right); \; \mathbf{u}_{pj} = \frac{Q_{pj} - A_{pj}}{\| Q_{pj} - A_{pj} \|}; \; j = 1, \cdots, 5 \tag{52f}$$

$$\omega_{pb}\mathbf{u}_{pb} = \omega_{pj}\mathbf{u}_{pj} - \omega_{bj}\mathbf{u}_{jb} \Rightarrow \frac{\omega_{pj}}{\omega_{bj}} = \frac{\mathbf{u}_{jb} \cdot \left(\mathbf{n}_j \times \mathbf{u}_{pb}\right)}{\mathbf{u}_{pj} \cdot \left(\mathbf{n}_j \times \mathbf{u}_{pb}\right)} = \frac{\mathbf{n}_j \cdot \left(\mathbf{u}_{jb} \times \mathbf{u}_{pb}\right)}{\mathbf{n}_j \cdot \left(\mathbf{u}_{pj} \times \mathbf{u}_{pb}\right)} = \frac{\left(\mathbf{u}_{jb} \times \mathbf{u}_{pb}\right)^2}{\left(\mathbf{u}_{jb} \times \mathbf{u}_{pb}\right) \cdot \left(\mathbf{u}_{pj} \times \mathbf{u}_{pb}\right)}; \; j = 1, \cdots, 5 \tag{52g}$$

where $\mathbf{i}_b$, $\mathbf{j}_b$, and $\mathbf{k}_b$ are the unit vectors of the co-ordinate axes x_b, y_b, and z_b, respectively; whereas, the linear variable a_{pb} and the three

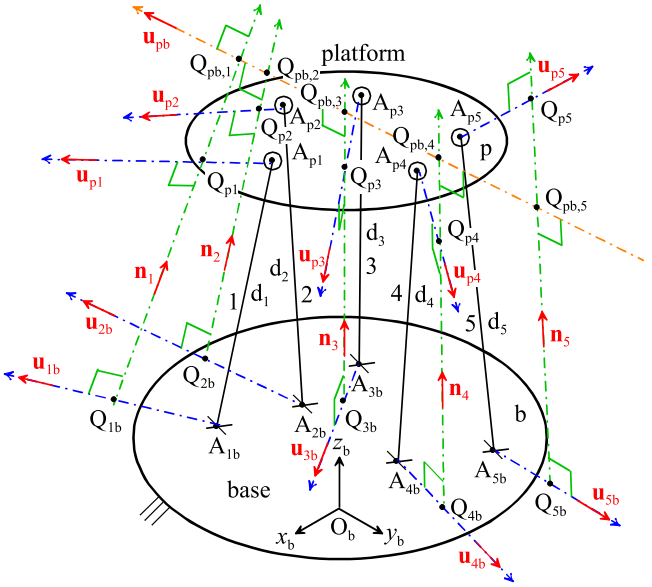

Fig. 12. Diagram of the 5-US mechanism that contains ISA_{pb} together with ISA_{pj} and ISA_{jb} for j=1, …,5 in a spatial disposition that satisfies Eqs. (52a)–(52f).

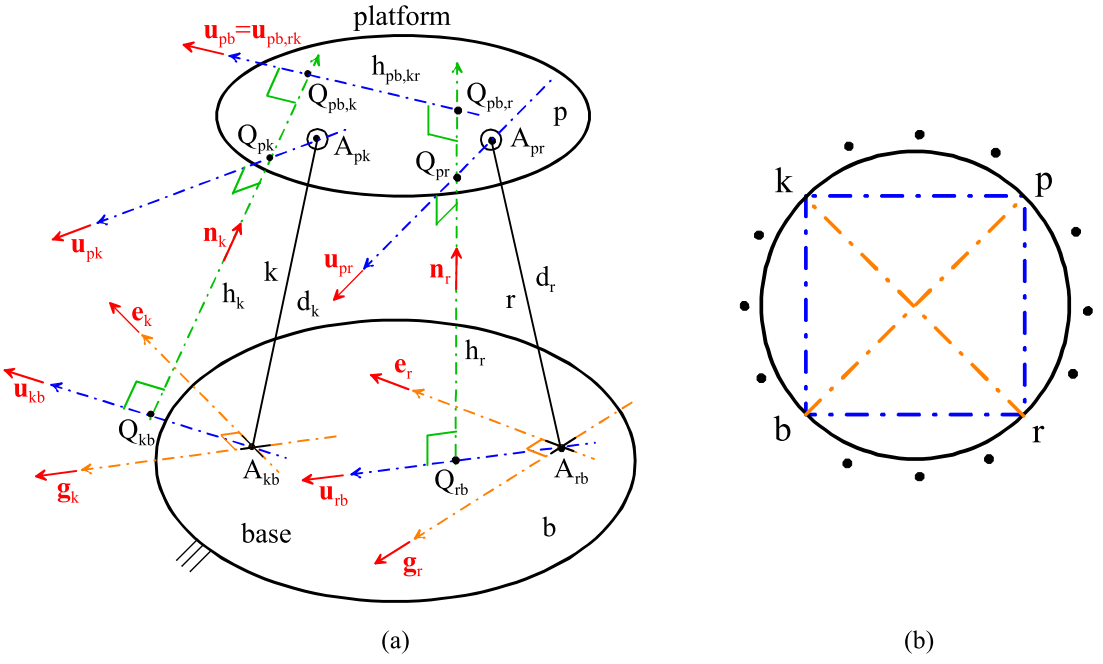

Fig. 13. Determination of ISA_{pb} through the four partially-known secondary ISAs associated to limb k and limb r: (a) geometric determination, (b) circle diagram (the blue dot-dash lines indicate these four partially-known ISAs; the brown dot-dash lines indicate the ISAs whose locations can be directly determined after these four partially-known ISAs have been located).

angular variables α_{pb}, β_{pb} and γ_{pb} are four unknowns whose determination uniquely locates $ISA_{pb}\equiv(A_{pb}, \mathbf{u}_{pb})$; eventually, the five angular variables β_{jb}, for j=1,…,5, are five more unknowns whose determination uniquely locates the five $ISA_{jb}\equiv(A_{jb}, \mathbf{u}_{jb})$, for j=1, …,5.

Eqs. (52a)–(52f) show that, once the above-mentioned nine unknowns have been determined, $ISA_{pb}\equiv(A_{pb}, \mathbf{u}_{pb})$ and the ten partially-known secondary ISAs (i.e., $ISA_{pj}\equiv(A_{pj}, \mathbf{u}_{pj})$ and $ISA_{jb}\equiv(A_{jb}, \mathbf{u}_{jb})$ for j=1,…,5) have been located. In addition, they show that the geometric conditions the EAK theorem imposes to the lines of these eleven ISAs can be satisfied by arbitrarily choosing nine variables (see Fig. 12). This is due to the fact that the uniqueness of the ISAs in single-DOF mechanism comes out when, over the geometric conditions highlighted by the EAK theorem, the geometric/kinematic relationships (Eqs. (8b) and (8c)) that have been

Table 2
Numerical example of a 5-US mechanism: numerical results (l.u. stands for generic length unit).

j	$\mathbf{u}_{jb}$ [l.u.]	Q_{jb} [l.u.]	$\mathbf{u}_{pj}$ [l.u.]	Q_{pj} [l.u.]	$Q_{pb,j}$ [l.u.]
1	(0.9197, −0.0239, −0.3919)^T	(0.1558, −0.0041, −0.0664)^T	(0.1469, 0.4379, −0.8870)^T	(0.1612, 0.0169, −0.0552)^T	(0.1947, 0.1489, 0.0155)^T
2	(0.9622, −0.2474, 0.1137)^T	(0.5245, −0.0723, 0.0332)^T	(0.8941, 0.2237, −0.3880)^T	(0.5332, −0.0133, 0.0875)^T	(0.5369, 0.0112, 0.1100)^T
3	(−0.9716, 0.1873, 0.1446)^T	(0.2986, 0.0888, 0.0373)^T	(0.1530, 0.4039, −0.9019)^T	(0.3085, 0.1262, 0.0557)^T	(0.3030, 0.1053, 0.0454)^T
4	(−0.0568, −0.9977, −0.0370)^T	(0.3882, 0.0702, 0.0755)^T	(0.8774, −0.4148, 0.2411)^T	(0.3041, 0.0640, 0.3710)^T	(0.3899, 0.0703, 0.0694)^T
5	(−0.8410, 0.0412, 0.5395)^T	(−0.0481, 0.2406, −0.0532)^T	(−0.2871, 0.4171, −0.8624)^T	(−0.0402, 0.2670, −0.0430)^T	(−0.0465, 0.2459, −0.0511)^T

deduced together with the demonstration of the EAK theorem in subSection 2.1 are satisfied, too.

In particular, the relative motion pb must be the same no matter which limb is used to determine it; therefore, the different expressions, $p_{pb,j}$ for j=1,…,5, of pitch p_{pb} of this motion that are computed by using Eq. (8b) with the data coming from different limbs must provide the same value. From an analytic point of view, this kinematic condition brings one to write the following four scalar equations in the above-mentioned nine unknowns

$$\begin{cases} p_{pb,1} = p_{pb,2} \\ p_{pb,1} = p_{pb,3} \\ p_{pb,1} = p_{pb,4} \\ p_{pb,1} = p_{pb,5} \end{cases} \tag{53}$$

with (see Eq. (8b) by reminding that the U-joints and the S-pairs impose p_{jb}=p_{pj}=0 for j=1,…,5)

$$p_{pb,j} = \frac{h_j \parallel \mathbf{u}_{pj} \times \mathbf{u}_{jb} \parallel \left(\frac{\omega_{pj}}{\omega_{bj}}\right)}{1 - 2\left(\frac{\omega_{pj}}{\omega_{bj}}\right)\left(\mathbf{u}_{pj} \cdot \mathbf{u}_{jb}\right) + \left(\frac{\omega_{pj}}{\omega_{bj}}\right)^2} = \frac{\left(A_{pj} - Q_{jb}\right) \cdot \left(\mathbf{u}_{pj} \times \mathbf{u}_{jb}\right)\left(\frac{\omega_{pj}}{\omega_{bj}}\right)}{1 - 2\left(\frac{\omega_{pj}}{\omega_{bj}}\right)\left(\mathbf{u}_{pj} \cdot \mathbf{u}_{jb}\right) + \left(\frac{\omega_{pj}}{\omega_{bj}}\right)^2}; j = 1, \cdots, 5 \tag{54}$$

where the expression of h_j given by Eq. (52e) has been used to deduce the last formula and the expressions of $(\omega_{pj}/\omega_{bj})$, for j=1,…,5, as a function of the geometric data are given by Eq. (52g).

Moreover, Eq. (8c) when applied to each limb brings one to write the following five more scalar equations in the same nine unknowns (see the first formula of Eq. (52e) and Eq. (8c) by reminding that the U-joints and the S-pairs impose p_{jb}=p_{pj}=0 for j=1,…,5)

$$\begin{aligned} \left(Q_{pb,j} - Q_{jb}\right) \cdot \mathbf{n}_j &= \frac{h_j\left[1 - \left(\frac{\omega_{pj}}{\omega_{bj}}\right)\left(\mathbf{u}_{pj} \cdot \mathbf{u}_{jb}\right)\right]}{1 - 2\left(\frac{\omega_{pj}}{\omega_{bj}}\right)\left(\mathbf{u}_{pj} \cdot \mathbf{u}_{jb}\right) + \left(\frac{\omega_{pj}}{\omega_{bj}}\right)^2} \Rightarrow \left(Q_{pb,j} - Q_{jb}\right) \cdot \left(\mathbf{u}_{jb} \times \mathbf{u}_{pb}\right) = \frac{\left(A_{pj} - Q_{jb}\right) \cdot \left(\mathbf{u}_{jb} \times \mathbf{u}_{pb}\right)\left[1 - \left(\frac{\omega_{pj}}{\omega_{bj}}\right)\left(\mathbf{u}_{pj} \cdot \mathbf{u}_{jb}\right)\right]}{1 - 2\left(\frac{\omega_{pj}}{\omega_{bj}}\right)\left(\mathbf{u}_{pj} \cdot \mathbf{u}_{jb}\right) + \left(\frac{\omega_{pj}}{\omega_{bj}}\right)^2}; \quad j \\ &= 1, \cdots, 5 \end{aligned} \tag{55}$$

where the expressions of $\mathbf{n}_j$ and h_j given by Eqs. (52c) and (52e), respectively, have been used to deduce the last formula and the expressions of $(\omega_{pj}/\omega_{bj})$, for j=1,…,5, as a function of the geometric data are given by Eq. (52 g).

Eqs. (53) and (55) constitute a system (compatibility system) of nine scalar equations in nine unknowns whose solution uniquely locates the sought-after ISA_{pb} and the ten partially-known ISAs. After having determined these eleven ISAs, the remaining ten secondary ISAs, which have not been determined, yet, are the ISA_{kr} with $r, k \in \{1, \ldots, 5 | r \neq k\}$ (here, it is worth stressing that the couples (r, k) are exactly ten (=5*(5–1)/2)). Such ten ISAs can be directly computed through the steps (i), (iii)–(v) of the algorithm presented in Section 2.3. Indeed, the four partially-known ISAs associated to two different limbs, that is (see Fig. 13(a)), ISA_{pk}, ISA_{kb}, ISA_{pr}, and ISA_{rb} with $r, k \in \{1, \ldots, 5 | r \neq k\}$, satisfy the conditions (i.e., rule 2) for the application of the FA theorem and the circle diagram associated to them (Fig. 13b) shows that, if they are fully located, they can be directly used to compute both ISA_{pb}, which has been already computed by solving the compatibility system, and the ISA_{kr} with $r, k \in \{1, \ldots, 5 | r \neq k\}$.

The above-reported formulas have been tested on a 5-US mechanism whose configuration is assigned through the following data (l.u. stands for generic length unit): A_{1b}=(0,0,0)^T l.u., A_{2b}=(0.243041, 0, 0)^T l.u., A_{3b}=(0.250015, 0.098196, 0.044518)^T l.u., A_{4b}=(0.391300, 0.124471, 0.077507)^T l.u., A_{5b}=(−0.130953, 0.244635, 0)^T l.u., A_{p1}=(0.108475, −0.140175, 0.263091)^T l.u., A_{p2}=(0.189570, −0.099235, 0.236663)^T l.u., A_{p3}=(0.270933, 0.026986, 0.277295)^T l.u., A_{p4}=(0.169728, 0.127555, 0.334066)^T l.u., A_{p5}=(0.096696, 0.068067, 0.368364)^T l.u.. Since the actual architectures of the U-joints are not of interest, the unit vectors $\mathbf{e}_j$ and $\mathbf{g}_j$ have been chosen both perpendicular to the axis of limb j, for j=1,…,5. With these data, the solution of the compatibility system (i.e., Eqs. (53) and (55)) provides the results reported in Table 2 and the following ISA_{pb}: A_{pb}=(0.082372, 0.194075, −0.015518)^T l.u., $\mathbf{u}_{pb}$=(0.898684, −0.361582, 0.248243)^T l.u., p_{pb}=−0.018114 lu. . Fig. 14 shows the 5-US mechanism together with the computed ISAs.

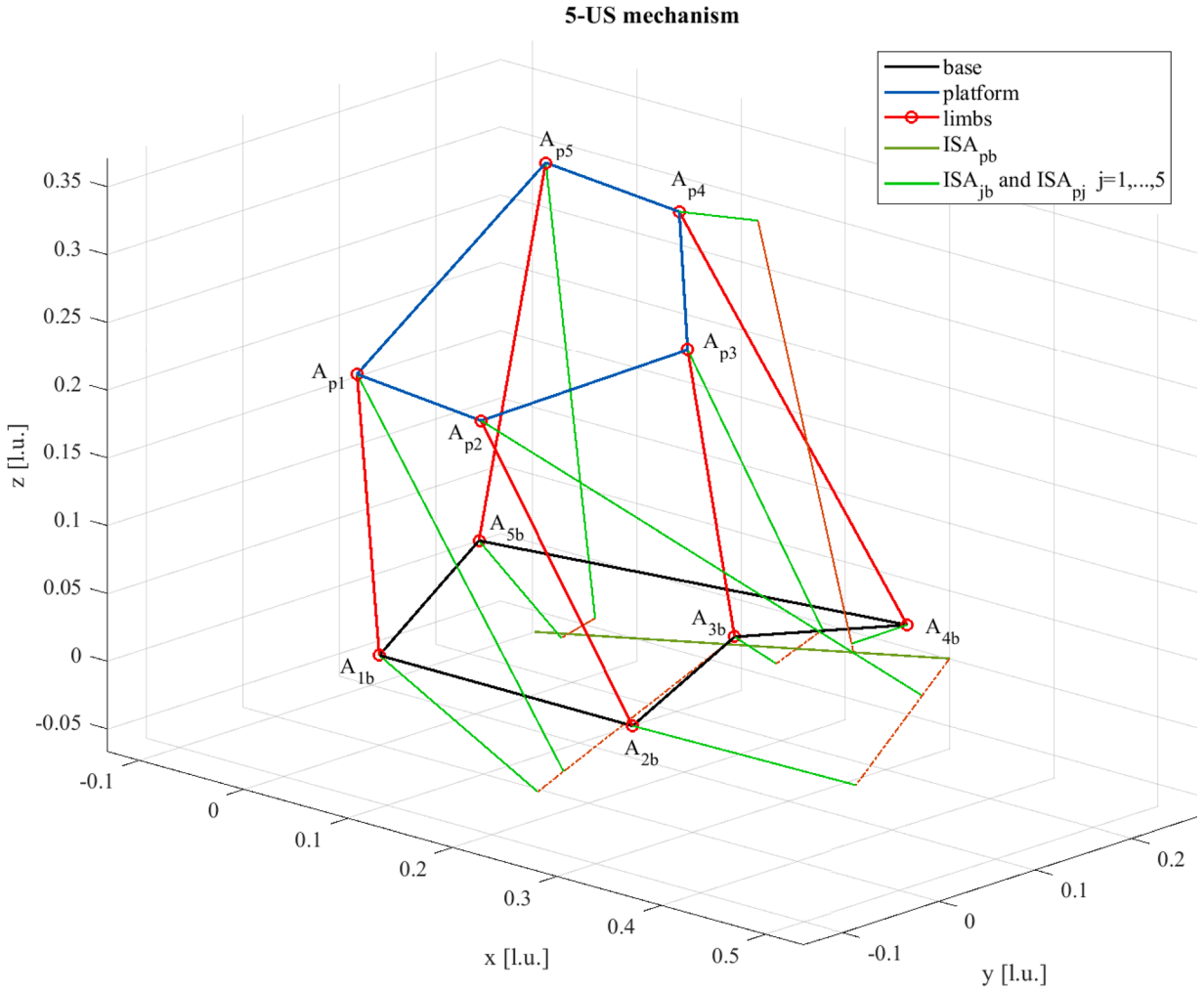

Fig. 14. Numerical example of a 5-US mechanism: diagram of the mechanism at the assumed configuration together with the computed ISAs.

4. Discussion

The algorithm proposed in Section 2.3 combines two parts: (a) steps (i), (iii)–(v) and (b) steps (vi)–(xii). Part (a) must be used (see step (ii)) when there is a sequence, which is obtainable through a circle diagram, of secondary ISAs that can be sequentially determined by directly using the EAK theorem. Part (b) must be used (see step (ii)) when a number of secondary ISAs need a simultaneous (i.e., not in sequence) determination through the introduction of unknowns and the solution of an equation system (compatibility system). These two parts are also present in the algorithms that compute the secondary ICs of planar mechanisms (see [9] for instance) and, by analogy with the planar case, the spatial single-DOF mechanisms that needs part (b) for the determination of their secondary ISAs can be named "indeterminate" mechanisms. Differently from the planar case, the majority of spatial single-DOF mechanisms are indeterminate even though they usually do not need the introduction of a high number of unknowns as in the case of the 5-US mechanism presented in Section 3.2. This is due to the fact that, differently from planar mechanisms, where the possible kinematic pairs are only four (i.e., R, P, R_P and S_P) with three of them that uniquely determine a primary IC, the possible kinematic pairs that are present in spatial mechanisms are ten (i.e., the one analyzed in Section 2.2) and only five (i.e., R, P, H, C, and R_L) of them bring to determine a primary ISA.

The implementation of part (a) is easy to automate since it simply consists in the reiterated use of the formulas reported in Section 2.1 after the sequence with which the secondary ISAs must be computed has been determined through a circle diagram. Differently, the implementation of part (b) uses the formulas of Section 2.1 to generate multiple symbolic expressions of the sought-after kinematic quantities; then, it obtains the equation system to solve by imposing the compatibility of different expressions of the same quantity. Thus, the implementation of part (b) requires an algebraic manipulator and a strategy for identifying the smallest set of equations to solve.

From a geometric point of view, the implementation of part (a) in a CAD system is direct; whereas, the implementation of part (b) requires a trial-and-error procedure that, by assigning trial values to the unknown data, tries to satisfy all the geometric and kinematic

conditions on the sought-after ISAs. The same difference occurs in the geometric determination of the ICs in planar single-DOF mechanisms when not-indeterminate and indeterminate linkages are considered [4,6,8]. Differently from the planar case, where all the pitches associated to the ISAs are equal either to 0 or to infinity, in the spatial case, where the same pitches can assume any real value, the determination of the secondary ISAs needs to consider also geometric/kinematic conditions (e.g., Eqs. (8b) and (8c)) that complement the EAK theorem and take into account the variability of the pitches.

The geometric determination of the ISAs does not change when a kinematic pair is replaced by another pair that provides the same geometric constraint on the ISA of the relative motion between the two links joined by that pair. For instance, in Fig. 8(a), replacing the R-pair with an H-pair (i.e., considering an HCCC mechanism instead of an RCCC mechanism) whose axis coincides with the axis of the replaced R-pair changes neither the locations of the secondary ISAs in the considered mechanism configuration nor the circle diagram of Fig. 8(b), even though it slightly affects the accompanying equations when the change of configuration is considered since point Q_{21} is no longer a fixed point of the frame (link 1) in the resulting HCCC mechanism. Moreover, since geometric changes of a mechanism that do not affect the ISAs' locations do not affect the mechanism motion near to the considered configuration (e.g., the reference configuration of a car suspension), drawing a mechanism diagram that contains all the ISAs (e.g., Figs. 8(a) and 12), as this approach brings to do, allows the identification of all the possible changes that do not affect the mechanism motion. For instance, in the case of the j-th limb of the 5-US mechanism (Fig. 9(b)), moving the limb's attachment point A_{jb} (A_{pj}) along $ISA_{jb}\equiv(A_{jb}, \mathbf{u}_{jb})$ (along $ISA_{pj}\equiv(A_{pj}, \mathbf{u}_{pj})$) does not change the location of ISA_{jb}, ISA_{pj} and ISA_{pb}, that is, does not change the mechanism motion near that configuration. Eventually, the classification, reported in Section 2.2, of the geometric conditions on the ISAs due to all the possible kinematic pairs combined with the proposed approach greatly facilitates the synthesis of a spatial single-DOF mechanism starting from the desired locations of the ISAs, that is, from the motion requirements. All these features make the proposed approach more appealing than others during mechanism design.

Finally, in Section 2.1, the possible VCs (see Eqs. (9), (17), and (18)) have been explicitly expressed as functions of the geometric parameters that identify the involved ISAs. As a consequence, the geometric construction obtained with the proposed approach, where all the ISAs are reported on the mechanism, immediately provides pieces of information that are relevant in evaluating both how the variation of the generalized coordinate affects the variations of all the other joint variables (i.e., the kinematic performance of the mechanism) and how the generalized torque that controls the generalized coordinate affects/equilibrates the other loads applied to the mechanism links (i.e., the static performance of the mechanism).

5. Conclusions

The spatial extension of the Aronhold-Kennedy (EAK) theorem has been combined with a corollary of the EAK theorem, named four-axes (FA) theorem, with geometric/kinematic conditions that complement the EAK theorem and with the taxonomy of the geometric constraints on instantaneous screw axes (ISAs) due to the kinematic pairs for devising a geometric and analytic technique that determines the ISAs directly from the mechanism configuration in single-DOF spatial mechanisms.

The proposed technique is the spatial extension of those techniques used for the determination of the instant centers (ICs) directly from the mechanism configuration in planar single-DOF mechanisms. In particular, as those techniques, it uses circle diagrams for finding the sequence with which the ISAs must be computed and, when the circle diagram is not able to find this sequence, it brings one to determine a system of equations (compatibility system) to solve for simultaneously determine a number of ISAs that restart the sequential determination.

A result of the analysis that supports the proposed technique is that "indeterminate" mechanisms are much more frequent among spatial single-DOF mechanisms than among planar single-DOF mechanisms. Despite this, the proposed geometric and analytic technique keeps many appealing features to exploit in mechanism design.

The proposed technique has been also applied to two relevant spatial single-DOF mechanisms: the RCCC mechanism and the 5-US parallel mechanism. As far as this author is aware, even though the background concepts involved in the formulation of the proposed approach are known, their combination into a self-standing procedure for the ISA determination is novel.

Declaration of Competing Interest

The authors declare that they have no known competing financial interests or personal relationships that could have appeared to influence the work reported in this paper.

Data availability

No data was used for the research described in the article.

Acknowledgments

This work has been developed at the Laboratory of Mechatronics and Virtual Prototyping (LaMaViP) of Ferrara Technopole, supported by FAR2021 UNIFE funds.

Appendix A

With reference to Fig. 3(a), let (A_{ji}, $\mathbf{u}_{ji}$) and (A_{ik}, $\mathbf{u}_{ik}$) be two skew lines, the following relationships hold:

$$\left.\begin{aligned} P_{ji} &= A_{ji} + \lambda \mathbf{u}_{ji} \\ P_{ik} &= A_{ik} + \mu \mathbf{u}_{ik} \end{aligned}\right\} \Rightarrow \left(P_{ji} - P_{ik}\right)^2 = \left[\left(A_{ji} - A_{ik}\right) + \lambda \mathbf{u}_{ji} - \mu \mathbf{u}_{ik}\right]^2 = f(\lambda, \mu) \tag{A.1}$$

where P_{ji} (P_{ik}) is a generic point of line (A_{ji}, $\mathbf{u}_{ji}$) (of line (A_{ik}, $\mathbf{u}_{ik}$))

The determination of the minimum of $f(\lambda, \mu)$ yields the values of λ and μ corresponding to Q_{ji} and Q_{ik} (see Fig. 3(a)). Such a minimum is determined by equating to zero the gradient of $f(\lambda, \mu)$, that is, by imposing $\nabla f(\lambda, \mu) = 0$, which yields the system

$$\begin{cases} \dfrac{\partial f}{\partial \lambda} = 2\left[\left(A_{ji} - A_{ik}\right) + \lambda \mathbf{u}_{ji} - \mu \mathbf{u}_{ik}\right] \cdot \mathbf{u}_{ji} = 2\left[\lambda - \mu \mathbf{u}_{ik} \cdot \mathbf{u}_{ji} + \left(A_{ji} - A_{ik}\right) \cdot \mathbf{u}_{ji}\right] = 0 \\ \dfrac{\partial f}{\partial \mu} = -2\left[\left(A_{ji} - A_{ik}\right) + \lambda \mathbf{u}_{ji} - \mu \mathbf{u}_{ik}\right] \cdot \mathbf{u}_{ik} = 2\left[\mu - \lambda \mathbf{u}_{ik} \cdot \mathbf{u}_{ji} - \left(A_{ji} - A_{ik}\right) \cdot \mathbf{u}_{ik}\right] = 0 \end{cases} \tag{A.2}$$

whose solution gives the following explicit formulas

$$\begin{cases} \lambda_{Q_{ji}} = \dfrac{\left(A_{ik} - A_{ji}\right) \cdot \left[\mathbf{u}_{ji} - \left(\mathbf{u}_{ik} \cdot \mathbf{u}_{ji}\right)\mathbf{u}_{ik}\right]}{1 - \left(\mathbf{u}_{ik} \cdot \mathbf{u}_{ji}\right)^2} \\ \mu_{Q_{ik}} = \dfrac{\left(A_{ji} - A_{ik}\right) \cdot \left[\mathbf{u}_{ik} - \left(\mathbf{u}_{ik} \cdot \mathbf{u}_{ji}\right)\mathbf{u}_{ji}\right]}{1 - \left(\mathbf{u}_{ik} \cdot \mathbf{u}_{ji}\right)^2} \end{cases} \tag{A.3}$$

The introduction of formulas (A.3) into the parametric equations of the two lines (i.e., Eqs. (A.1)) yields the following explicit expressions of the coordinates of Q_{ji} and Q_{ik}:

$$\begin{aligned} Q_{ji} &= A_{ji} + \frac{\left(A_{ik} - A_{ji}\right) \cdot \left[\mathbf{u}_{ji} - \left(\mathbf{u}_{ik} \cdot \mathbf{u}_{ji}\right)\mathbf{u}_{ik}\right]}{1 - \left(\mathbf{u}_{ik} \cdot \mathbf{u}_{ji}\right)^2}\mathbf{u}_{ji} = A_{ji} + \frac{\left(A_{ik} - A_{ji}\right) \cdot \left(\mathbf{u}_{ji} - \mathbf{u}_{ik}\cos\alpha_{ji,ik}\right)}{\sin^2\alpha_{ji,ik}}\mathbf{u}_{ji} \\ Q_{ik} &= A_{ik} + \frac{\left(A_{ji} - A_{ik}\right) \cdot \left[\mathbf{u}_{ik} - \left(\mathbf{u}_{ik} \cdot \mathbf{u}_{ji}\right)\mathbf{u}_{ji}\right]}{1 - \left(\mathbf{u}_{ik} \cdot \mathbf{u}_{ji}\right)^2}\mathbf{u}_{ik} = A_{ik} + \frac{\left(A_{ji} - A_{ik}\right) \cdot \left(\mathbf{u}_{ik} - \mathbf{u}_{ji}\cos\alpha_{ji,ik}\right)}{\sin^2\alpha_{ji,ik}}\mathbf{u}_{ik} \end{aligned} \tag{A.4}$$

where the relationship $\mathbf{u}_{ik} \cdot \mathbf{u}_{ji} = \cos\alpha_{ji,ik}$ (see Fig. 3(a)) has been used to write the last expressions.

It is worth noting that the relationships $(Q_{ji} - Q_{ik}) \cdot \mathbf{u}_{ji} = 0$ and $(Q_{ji} - Q_{ik}) \cdot \mathbf{u}_{ik} = 0$ are satisfied and that the distance, h, between the two skew line can be immediately computed through the following formula:

$$h = \left(Q_{ik} - Q_{ji}\right) = \left(A_{ik} - A_{ji}\right) \cdot \mathbf{n}_i \tag{A.5}$$

References

[1] J.H. Ginsberg, Advanced Engineering Dynamics, 2nd Ed., Cambridge University Press, New York NY, 1995.
[2] S. Aronhold, Gruendzuge der Kinematischen Geometrie, Verh. d. Ver. Z. Befoerderung des Gewerbeeiss in Preussen 51 (1872) 129–155.
[3] A.B.W. Kennedy, The Mechanics of Machinery, The MacMillan Company, London UK, 1886.
[4] A.W. Klein, Kinematics of Machinery, McGraw-Hill Book Company, Inc., New York, NY, USA, 1917.
[5] B. Paul, Kinematics and Dynamics of Planar Machinery, Prentice-Hall, Inc., Englewood Cliffs, NJ, USA, 1987.
[6] D.E. Foster, G.R. Pennock, A graphical method to find the secondary instantaneous centers of zero velocity for the double butterfly linkage, ASME J. Mech. Des. 125 (2003) 268–274.
[7] G.R. Pennock, E.C. Kinzel, Path curvature of the single flier eight-bar linkage, ASME J. Mech. Des. 126 (2004) 470–477.
[8] D.E. Foster, G.R. Pennock, Graphical methods to locate the secondary instantaneous centers of single-degree-of-freedom indeterminate linkages, ASME J. Mech. Des. 127 (2005) 249–256.
[9] R. Di Gregorio, An algorithm for analytically calculating the positions of the secondary instant centers of indeterminate linkages, ASME J. Mech. Des. 130 (2008), pp. 042303-(1:9).
[10] C.M. Kung, L.C.T. Wang, Analytical method for locating the secondary instant centers of indeterminate planar linkages, Proc. Ist. Mech. Eng. C-J. Mec. 223 (2009) 491–502.
[11] J.S. Beggs, Ein Beitrag zur Analyse raeumlicher Mechanismen, Technischen Hoechschule Hannover, 1959. PhD Dissertation.
[12] J.R. Phillips, K.H. Hunt, On the theorem of three axes in the spatial motion of three bodies, Austr. J. Appl. Sci. 15 (1964) 267–287.
[13] J.S. Beggs, Advanced Mechanisms, The MacMillan Company, New York NY, 1966.
[14] K.H. Hunt, Kinematic Geometry of Mechanisms, Oxford University Press, Oxford UK, 1978.
[15] O. Bottema, B. Roth, Theoretical Kinematics, Dover Publications, New York NY, 1979.
[16] J.S. Beggs, Kinematics, Hemisphere Publishing Company, Washington DC, 1983.
[17] J. Phillips, Freedom in Machinery, Volume 1 & Volume 2 Combined, Cambridge University Press, Cambridge UK, 1990.
[18] C.H. Suh, Differential displacement matrices and the generation of screw axis surfaces in kinematics, ASME J. Eng. Ind. 93 (1) (1971) 1–10, https://doi.org/10.1115/1.3427876. February.

[19] J.I. Valderrama-Rodríguez, J.M. Rico, J.J. Cervantes-Sánchez, F.T. Pérez-Zamudio, A New Look to the Three Axes Theorem, in: *Procs. of the ASME 2019 International Design Engineering Technical Conferences and Computers and Information in Engineering Conference, Vol. 5B: 43rd Mechanisms and Robotics Conference*, Anaheim, California, USA, 2019, https://doi.org/10.1115/DETC2019-97443. August 18–21, Paper No.: DETC2019-97443, V05BT07A062.
[20] J.I. Valderrama-Rodríguez, J.M. Rico, J.J. Cervantes-Sánchez, A general method for the determination of the instantaneous screw axes of one-degree-of-freedom spatial mechanisms, Mech. Sci. 11 (2020) 91–99, https://doi.org/10.5194/ms-11-91-2020.
[21] R. Beyer, New ways for graphic solution of spatial problems of mechanics, Uspekhi Mat. Nauk (7) (1940) 223–245, 1940 (in Russian).
[22] R. Beyer, Space mechanisms, in: Trans. of the 5th Conf. on Mechanisms, Cleveland, Ohio (USA), Purdue University, Penton Publishing Co., 1958, pp. 141–163.
[23] R. Beyer, Technische Raumkinematik, Springer-Verlag, Berlin, Germany, 1963.
[24] J. Phillips, Determination of Instantaneous Screw Axes in Spatial Mechanism, in: Procs of the Int. Conf. on Mechanisms and Machines, Varna, Bulgaria I, 1965, pp. 245–269.
[25] G. Figliolini, P. Rea, J. Angeles, The synthesis of the axodes of RCCC linkages, J. Mech. Robot. 8 (2) (2016), 021011, https://doi.org/10.1115/1.4031950.
[26] M.D. Ardema, Newton-Euler Dynamics, Springer, New York, NY, 2005.
[27] L.O. Barton, Mechanism Analysis: Simplified Graphical and Analytical Techniques, Marcel Dekker Inc., New York, NY, USA, 1993. ISBN 9780429102493.
[28] A. Kumar-Mallik, A. Ghosh, G. Dittirich. Kinematic Analysis and Synthesis of Mechanisms, CRC, Boca Raton, FL, USA, 1994.
[29] X. Wang, L. Baron, Topology and Geometry of Serial and Parallel Manipulators, in: Jee-Hwan Ryu (Ed.), Parallel Manipulators: New Developments, IntechOpen, London (UK), 2008, pp. 57–74, https://doi.org/10.5772/5363.
[30] C.H. Suh, C.W. Radcliffe, Kinematics and Mechanism Design, John Wiley & Sons, Inc., New York, NY, USA, 1978. ISBN: 9780471014614.
[31] R.I. Jamalov, F.L. Litvin, B. Roth, Analysis and design of RCCC linkages, Mech. Mach. Theory 19 (4–5) (1984) 397–407, https://doi.org/10.1016/0094-114X(84)90098-3.
[32] S. Dhall, S.N. Kramer, Design and analysis of the HCCC, RCCC, and PCCC spatial mechanisms for function generation, ASME J. Mech. Des. 112 (1) (1990) 74–78, https://doi.org/10.1115/1.2912582.
[33] S.D. Marble, G.R. Pennock, Algebraic-geometric properties of the coupler curves of the RCCC spatial four-bar mechanism, Mech. Mach. Theory 35 (5) (2000) 675–693, https://doi.org/10.1016/S0094-114X(99)00039-7.
[34] E. Pennestrì, R. Stefanelli, Linear algebra and numerical algorithms using dual numbers, Multibody Syst. Dyn. 18 (2007) 323–344, https://doi.org/10.1007/s11044-007-9088-9.
[35] C. Suh, Synthesis and analysis of suspension mechanisms with use of displacement matrices, SAE Technical Paper 890098, (1989) 189-200, doi: 10.4271/890098.
[36] C.H. Suh, Suspension analysis with instant screw axis theory, SAE Technical Paper 910017, (1991) 143–151. doi: 10.4271/910017.
[37] M. Hiller, Five-point wheel suspension, in: J. Angeles, A. Kecskemethy (Eds.), Kinematics and Dynamics of Multibody Systems, Springer, Berlin, Germany, 1995, pp. 177–188, https://doi.org/10.1007/978-3-7091-4362-9.
[38] C. Innocenti, Polynomial Solution of the Spatial Burmester Problem, ASME. J. Mech. Des. 117 (1) (1995) 64–68, https://doi.org/10.1115/1.2826118.
[39] M. Raghavan, Number and dimensional synthesis of independent suspension mechanisms, Mechanism Mach. Theory 31 (8) (1996) 1141–1153, https://doi.org/10.1016/0094-114X(96)84605-2.
[40] P.A. Simionescu, D.G. Beale, Synthesis and analysis of the five-link rear suspension system used in automobiles, Mechanism Mach. Theory 37 (9) (2002) 815–832, https://doi.org/10.1016/S0094-114X(02)00037-X.
[41] P.A. Simionescu, A unified approach to the kinematic synthesis of five-link, four-link, and double-wishbone suspension mechanisms with rack-and-pinion steering control, Proc. IMechE, Part D: J. Automobile Eng. 231 (10) (2017) 1374–1387, https://doi.org/10.1177/0954407016672775.
[42] V. Parenti-Castelli, A. Leardini, R. Di Gregorio, J.J. O'Connor, On the modeling of passive motion of the human knee joint by means of equivalent planar and spatial parallel mechanisms, Auton. Robots 16 (2004) 219–232, https://doi.org/10.1023/B:AURO.0000016867.17664.b1.
[43] V. Parenti-Castelli, Classification and Kinematic Modelling of Fully-Parallel Manipulators — A Review, in: C.R. Boër, L. Molinari-Tosatti, K.S. Smith (Eds.), Parallel Kinematic Machines: Theoretical Aspects and Industrial Requirements, Springer, London, UK, 1999, pp. 51–68, https://doi.org/10.1007/978-1-4471-0885-6_4.
[44] J.P. Yin, C.G. Liang, The forward displacement analysis of a kind of special platform manipulator mechanisms, Mech. Mach. Theory 29 (1) (1994) 1–9, https://doi.org/10.1016/0094-114X(94)90015-9.
[45] J. Nielsen, B. Roth, The direct kinematics of the general 6-5 stewart-gough mechanism, in: J. Lenarcic, V. Parenti-Castelli (Eds.), Recent Advances in Robot Kinematics, Springer, Dordrecht, The Netherlands, 1996, pp. 7–16, https://doi.org/10.1007/978-94-009-1718-7_1, 1996.
[46] C. Innocenti, A new algorithm for the direct kinematics of the 6–5 fully-parallel manipulator, in: Procs. of the 5th Appl. Mechanisms & Robot. Conf., Cincinnati, OH (USA), 1997. Paper No.: AMR97-039.
[47] V.S. Ryaben'kii, S.V. Tsynkov, A Theoretical Introduction to Numerical Analysis, CRC Press, London, UK, 2007.